TECHNISCHE UNIVERSITÄT WIEN

MASTER THESIS

# 60 GHz WIFI as Autonomous Cruise Control

*Author:*
Sergio Jiménez Gómez

*Advisor:*
Univ.Prof. Dr.techn. Markus Rupp
Univ.Ass. Dipl.-Ing. Erich Zöchmann

*Institute of Telecommunications (ITC)*
*Technische Universität Wien, Austria*

July 28, 2017

Technische Universität Wien

# *Abstract*

**60 GHz WIFI as Autonomous Cruise Control**

by Sergio Jiménez Gómez

The aim of this Master thesis is proving the feasibility of the standard IEEE 802.11ad to operate in a vehicular environment. The importance of the applications tested in this thesis is meaningful to increase the safety conditions at roads.

The transmitter was implemented according to the IEEE 802.11ad standard. The transmitter and the receiver are tested in several environments, where the main problem is to extract useful information, such as the position or the vehicles speed from the environment and share that information to increase safety. The tests show that the variety of modulation and coding schemes and the autocorrelation properties of the signals let the system offer a wide variety of throughputs guarantying the detection properties of the system and, therefore, assuring the collection of reliable information about the speed and the position of the vehicles.

The results seem promising for this applications concluding that 802.11ad is a good candidate for being a vehicular communication solution.

# *Acknowledgements*

Firstly, I would like to thank my thesis advisor Univ.Prof. Dr.techn. Markus Rupp of the Institute of Telecommunications at Technische Universität Wien and Univ.Ass. Dipl.-Ing. Erich Zöchmann. Their office was always open whenever I ran into a trouble spot or had a question about my research or writing. They consistently allowed this paper to be my own work, but steered me in the right direction, whenever they thought I needed it.

I would also like to thank the experts who were involved in the progress of this project: Dr.techn. Sebastian Caban, Dipl.-Ing. Martin Lerch, Dipl.-Ing. Stefan Pratschner, Dipl.-Ing. Ronald Nissel, and Bashar Tahir, B.Sc. Without their participation and input, this thesis could not have been successfully conducted.

I would also like to thank my parents and sister. They were always supporting me and encouraging me with their best wishes. I would also like to thank Juli Kainz, she was there cheering me up and stood by me through the good times and the bad.

Finally, I must express my very profound gratitude to Maria, Alvaro, Felix, Viki, Pati and my Erasmus friends for providing me with unfailing support and continuous encouragement throughout my years of study and through the process of researching and writing this thesis. This accomplishment would not have been possible without them. Thank you!

# Contents

**Abstract** iii

**Acknowledgements** v

**1 Introduction** 1

**2 Transmitter** 5
2.1 PHY Layers . . . 5
2.2 Control Layer (CL) . . . 6
2.2.1 Preamble generation . . . 6
2.2.2 Header and payload coding . . . 6
2.2.3 Modulation mapping . . . 8
DBPSK Modulation . . . 8
2.2.4 Spread Spectrum . . . 8
2.3 Single Carrier (SC) . . . 8
2.3.1 Preamble generation . . . 8
2.3.2 Header encoding . . . 9
2.3.3 Data encoding . . . 10
2.3.4 Modulation mapping . . . 10
$\frac{\pi}{2}$ - BPSK Modulation . . . 10
$\frac{\pi}{2}$ - QPSK Modulation . . . 11
$\frac{\pi}{2}$ - 16-QAM Modulation . . . 11
2.4 Low Power Single Carrier (LPSC) . . . 11
2.4.1 Preamble generation . . . 11
2.4.2 Header encoding . . . 11
2.4.3 Data encoding . . . 12
2.5 Orthogonal Frequency-Division Multiple (OFDM) access . . . 12
2.5.1 Preamble generation . . . 12
2.5.2 Header encoding . . . 12
2.5.3 Data encoding . . . 14
2.5.4 Modulation mapping . . . 14
SQPSK Modulation . . . 14
QPSK Modulation . . . 14
16-QAM Modulation . . . 15
64-QAM Modulation . . . 15
2.5.5 OFDM symbol . . . 15
2.5.6 Technique to reduced PAPR in OFDM . . . 17

**3 Receiver** 19
3.1 Signal detection & ranging . . . 19
3.1.1 Payload autocorrelation vs preamble autocorrelation . . . 19
3.1.2 Delay calculation . . . 21
3.2 Signal decoding . . . 21

3.2.1 Control layer (CL) . . . 21
Demodulation mapping . . . 22
Metrics and constellation . . . 22
3.2.2 Single Carrier (SC) . . . 23
Demodulation mapping . . . 25
Metrics and constellation . . . 26
3.2.3 Low Power Single Carrier (LPSC) . . . 27
Metrics and constellation . . . 30
3.2.4 Orthogonal Frequency-Division Multiple (OFDM) access . . . 30
Demodulation mapping . . . 30
Metrics and constellation . . . 33
3.2.5 OFDM Demodulation . . . 35

**4 Simulations** **37**
4.1 Individual tests . . . 37
4.1.1 Modulator/demodulators . . . 37
4.1.2 Coders . . . 37
4.1.3 Scrambler . . . 38
4.1.4 Interleaver . . . 38
4.1.5 Channel estimation . . . 38
4.1.6 Equalization . . . 40
4.2 System tests . . . 41
4.2.1 Detection . . . 41
4.2.2 Ideal data transmission . . . 43
4.2.3 AWGN channel transmission . . . 44

**5 Measurements** **49**
5.1 Setup . . . 49
5.2 Setting parameters . . . 49
5.2.1 Recording length . . . 49
5.2.2 Output frequency . . . 50
5.2.3 Sample frequency . . . 50
5.2.4 Input power level . . . 50
5.2.5 Signal Packets . . . 51
5.2.6 Attenuation values . . . 51
5.2.7 Trigger level . . . 51
5.3 Experiments . . . 51
5.3.1 Signal measurement procedure . . . 51
5.3.2 Data transmission measurements . . . 52
5.3.3 Radar measurements . . . 53

**6 Conclusion** **57**

**7 Bibliography** **59**

**A Scramble, demodulation, and Checksum** **61**
A.1 Scrambling . . . 61
A.1.1 Scramble part . . . 61
A.1.2 Descramble part . . . 61
A.2 Demodulation . . . 61
A.3 Checksum . . . 62

**B Evaluation of the transmitter. Metrics** **63**
B.1 CL . . . 63
B.2 SC . . . 63
B.3 OFDM . . . 63
B.4 Average constellation power . . . 64

**C Golay sequences** **65**
C.1 Guard Insertion . . . 65
C.1.1 LPSC . . . 65
C.1.2 SC . . . 65

**D Codification** **67**
D.1 LDPC coding/decoding . . . 67
D.1.1 Encoding . . . 67
D.1.2 Decoding . . . 68
D.2 Reed Solomon (N,K) . . . 69
D.2.1 Encoding . . . 70
D.2.2 Decoding . . . 70
D.3 Block code (8,N) . . . 71
D.3.1 Encoding . . . 71
D.3.2 Decoding . . . 72

**E Transmission procedures** **73**
E.1 Spectrum Matching . . . 73
E.1.1 OFDM . . . 73
E.1.2 CL, SC, and LPSC . . . 73
E.2 Quantization and Packets Generation . . . 73
E.3 Resampling . . . 74

**F Modulations** **75**

# List of Figures


1.1 Applications scheme . . . . . 3

2.1 PHY layers structure . . . . . 6
2.2 CL preamble structure . . . . . 6
2.3 CL Header structure . . . . . 7
2.4 SC preamble structure . . . . . 9
2.5 SC Header structure . . . . . 10
2.6 OFDM preamble structure . . . . . 13
2.7 OFDM Header structure . . . . . 13
2.8 OFDM clipping simulations (arctangent window) . . . . . 18

3.1 Applications scheme. . . . . 19
3.2 EVM CL . . . . . 23
3.3 EVM CL -15 dB. . . . . 24
3.4 EVM CL 0 dB. . . . . 24
3.5 Descramble Scheme . . . . . 25
3.6 EVM SC . . . . . 27
3.7 EVM SC 0 dB. . . . . 28
3.8 EVM SC 20 dB. . . . . 28
3.9 EVM LPSC 0 dB. . . . . 31
3.10 EVM LPSC 20 dB. . . . . 31
3.11 EVM OFDM . . . . . 33
3.12 EVM OFDM 0 dB. . . . . 34
3.13 EVM OFDM 20 dB. . . . . 34

4.1 Modulation schemes BER curves . . . . . 38
4.2 Reed Solomon and BC BER curves . . . . . 39
4.3 Channel estimation performance . . . . . 40
4.4 OFDM equalizer performance . . . . . 41
4.5 Preamble autocorrelation and Signal Detection Probability Preamble detection . . . . . 44
4.6 Payload autocorrelation and Signal Detection Probability Payload detection . . . . . 44
4.7 SC, LPSC, and OFDM physical layer performance. . . . . 45
4.8 Missed packets in SC, LPSC, and OFDM physical layers. . . . . 46
4.9 CL physical layer performance. . . . . 47

5.1 Setup scheme. . . . . 50
5.2 Relationship SINR/ATT . . . . . 53
5.3 4-QAM Constellation . . . . . 54
5.4 BER curves and Missed Packets for SC - Radar application . . . . . 55
5.5 BER curves and Missed Packets for OFDM - Radar application . . . . 55

A.1 CRC Block diagram . . . . . 62

D.1 LDPC correction procedure . . . . . 68

E.1 Resampling scheme . . . . . 74

F.1 DBPSK constellation . . . . . 75
F.2 $\frac{\pi}{2}$ - QPSK constellation . . . . . 75
F.3 $\frac{\pi}{2}$ - 16-QAM constellation . . . . . 76
F.4 64-QAM constellation . . . . . 76

# List of Tables

2.1 Pilot subcarrier location . . . . . 16
2.2 Data subcarrier location . . . . . 16

D.1 Word sizes per coding rate . . . . . 67

# List of Abbreviations

| | |
|---|---|
| **AGC** | **A**utomatic **G**ain |
| **AM** | **A**mplitude **M**odulation |
| **AWGN** | **A**dditive **W**hite **G**aussian **N**oise |
| **BC** | **B**lock **C**ode |
| **BER** | **B**it **E**rror **R**ate |
| **BPSK** | **B**inary **P**hase **S**hift **K**eying |
| **CE** | **C**hannel **E**stimation |
| **CL** | **C**ontrol **L**ayer |
| **CRC** | **C**yclic **R**edundancy **C**heck |
| **DSSS** | **D**irect **S**equence **S**pread **S**pectrum |
| **EVM** | **E**rror **V**ector **M**agnitude |
| **FFT** | **F**ast **F**ourier **T**ransform |
| $G_X$ | **G**olay (sequence a or b) |
| **HCS** | **H**eader **C**heck**S**um |
| **IFFT** | **I**nverse **F**ast **F**ourier **T**ransform |
| **LDPC** | **L**ow **D**ensity **P**arity **C**heckcode |
| **LFSR** | **L**inear **F**eedback **S**hift **R**egister |
| **LLR** | **L**og **L**ikelihood **R**atio |
| **LPSC** | **L**ow **P**ower **S**ingle **C**arrier |
| **LSB** | **L**east **S**ignificant **B**it |
| **MCS** | **M**odulation (and) **C**oding **S**cheme |
| **MSB** | **M**ost **S**ignificant **B**it |
| **MSE** | **M**ean **S**quared **E**error |
| **NGI** | **N**ormal **G**uard **I**nterval |
| **OFDM** | **O**rthogonal **F**requency **D**ivision **M**ultiplexing |
| **M-QAM** | M **Q**uadrature **A**mplitud **M**odulation (X) |
| **QPSK** | **Q**uadrature **P**hase **S**hift **K**eying |
| $P_d$ | **P**robability (detection) |
| $P_{fa}$ | **P**robability (false alarm) |
| **RS** | **R**eed **S**olomon |
| **RMS** | **R**oot **M**ean **S**quare |
| **ROC** | **R**eceiver **O**perating **C**haracteristic |
| **RRC** | **R**oot **R**aised **C**osine |
| **SC** | **S**ingle **C**arrier |
| **SINR** | **S**ignal (to) **I**nterference (plus) **N**oise **R**atio) |
| **SNR** | **S**ignal (to) **N**oise **R**atio |
| **SQPSK** | **S**pread **Q**uadrature **P**hase **S**hift **K**eying |
| **STF** | **S**hort **T**raining **F**ield |
| **TR** | **T**ransition **R**egion |
| **TRN** | **TR**ai **N**ing (field) |

# Physical Constants

Number of Data subcarriers $N_{sd} = 336$
Number of Pilot subcarriers $N_{sp} = 16$
Number of DC subcarriers $N_{dc} = 3$
Total subcarriers $N_{st} = 355$
Carriers occuping half of the bandwith $N_{sr} = 177$
OFDM sample rate $f_s = 2640MHz$
SC/CL chip rate $f_c = 1760MHz$
FFT size $S_{fft} = 512$

# Chapter 1

# Introduction

Wireless communications will always demand more throughput than what currently is available. Especially when several users must share the same physical resources, only a fraction of the nominal throughput remains. This also happens in vehicular environments. Data transmission between vehicles and ranging detection are functionalities required in nowadays society.

Communications between vehicles is a growing area. The advances in wireless communications are making it possible to share information through real time communications between vehicles. This has led to applications which increase safety of vehicles and communication between passengers, such as ranging applications to detect other vehicles or data transmission [3][8]. Standardization efforts on vehicular communication are also underway to make vehicular transportation safer, greener and easier. The usage of the applications presented either radar and data transmission are attractive, even when they are not designed for the same challenges. However, together they offer advantages in terms of cost, size, performance, and spectrum usage. These applications would be as a first step toward autonomous detection of the environment to no driver conduction and data exchanging to reduce transportation congestion, entertainment, and velocity and brake information. Consequently, it is an important development for automotive industry regarding safety and entertainment aspects.

The 60 GHz frequency range is unlicensed and available everywhere in the world and offers higher bandwidth channels for greater throughput and devices are more compact due to the small wavelength (approx. 5 mm). However, this frequency range is associated to a high attenuation values and oxygen absorption [4]. Consequently, the operation range is not high (10 - 100 m typically) avoiding channel interferences and data interception.

The frequency band proposed (60 GHz) seems a promising candidate to fulfill the functionalities presented in this project. Compact systems with low range and low consumption fit in a device like a car with limited space. The 802.11 WLAN standard has also been continuously updated to permit higher throughput. The latest developments are known as Very High Throughput (VHT) enhancement and are specified in two new amendments. One of those amendments is 11ad which covers the frequency range at 60 GHz. Therefore, the protocol 802.11ad is chosen to tackle the thesis. This standard presents several modes of transmission which cover several ranges of data rates and power consumption characteristics. It also provides higher data rate for communications and better accuracy and resolutions for radar operation, thus simultaneously achieving ultra-low latency and high range of operation for automotive safety applications. Moreover, 802.11ad is an IEEE standard which is

worldwide spread. Consequently, there is competence in developing the technology.

The problems treated in this document are intended to assess the reliability of this protocol in vehicles environments to offer ranging and data transmission functionalities.

- Chapter 2: A transmitter is programmed, this transmitter is able to pack the information in 3 PHYs which are compulsory in the standard and 1 extra physical layer which is optional.

- Chapter 3: The correspondent receiver is implemented. The receiver has two tasks. On the one hand, the receiver is able to detect signals and determines the transmission delay in order to use it as a radar to infer the distance to different vehicles. On the other hand, the receiver is able to decode signals to extract the information of the packet.

- Chapter 4: Packets for all possible modulation and coding schemes are generated and tested in the receiver to infer the behavior of the transponder in an AWGN channel with different SNR values. ROC (Receiver Operating Characteristic) curves are also simulated to infer the detection and false alarm probability of the system extracting reliability information.

- Chapter 5: The generated packets are loaded into an arbitrary waveform generator to test them in a real channel. Attenuating the signal, different self-interference and noise environments can be tested. The received packets are sampled as it is standardized and equalized. This procedure involves channel estimation per transmission and zero forcing equalization.

The project is tackled by simulating how the 802.11ad physical layer transports the data through an AWGN channel and the main objectives to achieve are summarize in the following points:

- Implementation of the 802.11ad transmitter and the receiver to transmit data between vehicles. the coding and decoding procedure of the signal following the 802.11ad specifications could make data transmission available in a mobile environment with a high range of possible throughputs. The functionality is tested through simulations and real measurements.
- Implementation of the signal detection based on the preamble fields of the packet structure or known payload for radar applications.
- Investigating how the characteristics of the data transmitted affects the detection properties. The data transmitted is known in the receiver and the data sequence could be longer that the packet preambles. Consequently, the autocorrelation properties of the signal could perform better for the signal detection problem. This objective is tackled with simulations.

The project is developed based on two different scenarios. The first scenario contemplates that one car is equipped with 802.11ad devices, therefore, it can execute

every application developed, but the second car is not equipped with the 802.11ad device and it is not able to execute the applications. The second scenario contemplates that all cars are equipped with 802.11ad devices and they can execute all the applications. The first (a) and second (b) scenarios can be observed in the Figure 1.1.

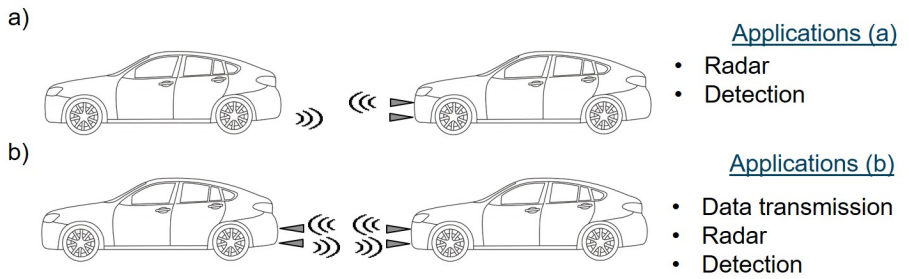


FIGURE 1.1: Applications scheme.

In this thesis, 30 MCS are tested in 100 noise realizations and 30 packs of signals to test the performance of the system. Furthermore, the former applications are tested in real environments at channel 3 at 62.64 GHz using the 4 less encoded MCS proposed by 802.11ad standard simulated in 3000 different SNR scenarios and different environments in a measurement setup.

Summarizing, the project is intended to prove that a telecommunication system based on the protocol 802.11ad is able to establish communication link between several vehicles with different throughputs and reliability levels. It must be able to obtain information from the environment such as the distance with different obstacle like other vehicles to increase safety of the passengers. To prove that these objectives are possible the system and the individual modules are tested.

# Chapter 2

# Transmitter

The transmitter part is a subsystem which is intended to pack the information which is sent following the 802.11ad requirements.

The 802.11ad transmitter accomplishes multiple tasks which are described a long this section. The transmitter is able to pack the information in 32 different MCS spread in 4 different PHY (Physical Layers). These 4 PHYs or modes are a Control Layer (CL) which is intended to exchange signaling and/or control messages in order to establish and monitor connections between the various devices. The Single Carrier (SC) mode transmits information through one carrier in a range of 385 Mbits/s to 4.26 Gbit/s depending on one of the 12 MCS. The OFDM mode is implemented in order to reach rates in a range of 693 Mbits to 6.757 Gbit/s. Additionally, an extra optional SC mode is included, this mode implements energy-saving encoders and it is called Low Power Single Carrier (LPSC) mode.

The 4 modes presented are formed by a similar structure with several fields. However, each mode implements each field differently. Those fields are:

- Preamble: The preamble consists of the Short Training Field (STF) and the Channel Estimation (CE) field. It is required in every packet. It supports the receiver during Automatic Gain Control (AGC), when recognizing the packet and in estimating frequency offset, and it displays the type of PHY that is used (SC or OFDM). The receiver also uses the known CE field to estimate the channel.
- Header: The header is different for every PHY and contains information for the receiver, such as the MCS, the length of the data field or the checksum.
- Data: This part is used to transmit the actual data with different MCS. The length of the field is variable.
- TRN: This field is optional and can be appended to all packets. It includes beamforming information. This field is not implemented in this project.

## 2.1 PHY Layers

As it was presented in the introduction of this section, 4 modes are implemented following a fixed structure. However, the fields of the packet structure are implemented differently depending on the mode and the MCS. The structure of the PHY is shown in the Figure 2.1.

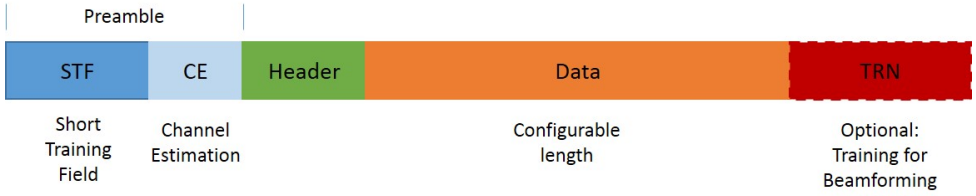


FIGURE 2.1: PHY layers structure.

Header parameters configure the properties of this specific layer. These parameters are the length of the payload, the MCS, and the scramble initial state. The length limit of the packet in simulations is 1023 octets, which is the length established in order to make the simulations as accurate as possible.

## 2.2 Control Layer (CL)

The Control Layer PHY is intended to send signaling to the receiver. It must be robust in order to establish a communication link between the transmitter and the receiver in low SNR conditions. This mode only has one MCS (MCS 0) which has strong coding and BPSK modulation.

### 2.2.1 Preamble generation

The preamble is generated using Golay sequences explained in section. The preamble is formed appending 50 Gb128 (Golay sequence b) symbols sequences. A Gb128 symbols sequence is repeated 48 times followed by –Gb128 and –Ga128 (Golay sequence a) symbols sequences. As a result, a 6400 symbols sequence is generated. The CE field is formed by 2 different 512 long symbols sequences. The Gu512 and Gv512 sequences are formed by combinations of Ga128 and Gb128 resulting in an 1152 symbols sequence. The preamble structure for CL is shown in Figure 2.2.

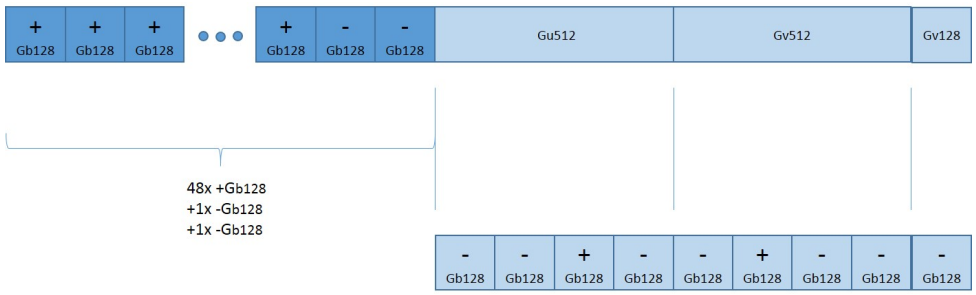


FIGURE 2.2: CL preamble structure.

### 2.2.2 Header and payload coding

- The header consists of 64 bits. The header structure is shown in Figure 2.3.
  - Scrambler initialization: It provides the start point for the scrambler.

- Length (data): It specifies the length of the data field. The range is 14 octets to 1023 octets.
- Packet type: It specifies whether the beamforming training field is intended for the receiver or the transmitter. It carries no information when Training Length = 0 and it is not necessary for this project since only one antenna is used.
- Training length: It specifies the length of the beamforming training field.
- Turnaround: It specifies communication settings between transmitter and receiver and it is not necessary for this project since only one antenna is used.
- HCS: It provides a checksum per CRC for the header.
- 3 bits (position 1 and position 23 and 24) are reserved.
- CRC is generated as it is indicated in the Appendix A.

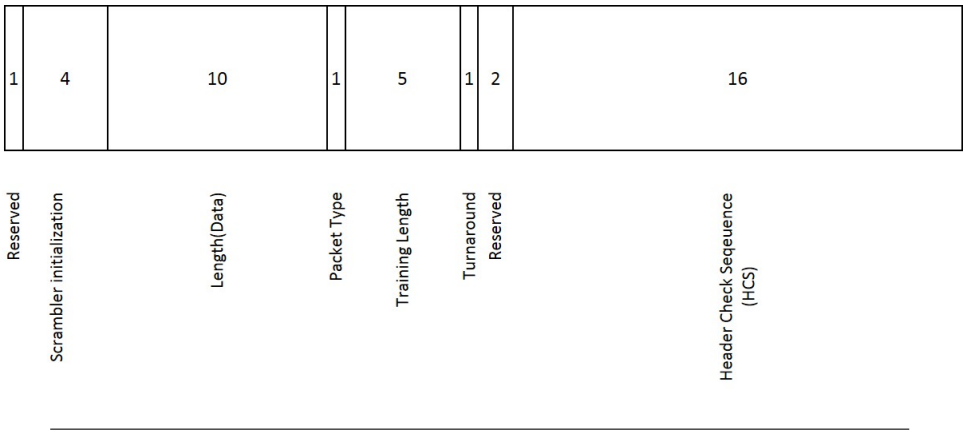


FIGURE 2.3: CL Header structure.

- Header and payload concatenation: The header and the payload are concatenated since both fields are encoded together.
  - Scramble with the sequence generation: The scramble procedure is done using the initial state established in the header. It is explained in the Appendix A.1.1.
  - LDPC encoding: The LDPC codification is accomplished with a $\frac{1}{2}$ coding rate [1]. It is explained in the Appendix D.1.1.
  - DPSK: Differential modulation is used due to its better performance than other 1 bit modulations. It is explained in 2.2.3.
  - Spreading: After encoding the signal, Direct Sequence Spread Spectrum (DSSS) spread using a Ga32 sequence is performed. It is explained in 2.2.4.
  - Filtering: The 802.11ad spectrum mask filtering is required. Consequently, a (RRC) Root Raised Cosine filter is applied in order the smooth the signal transition between symbols. It is explained in the Appendix E.1.2.

### 2.2.3 Modulation mapping

#### DBPSK Modulation

The input bit stream is converted into a stream of complex constellation points using differential binary phase shift keying (DBPSK). The differential sequences are generated using the following function:

$$d(k) = s(k)d(k-1) \tag{2.1}$$

The differential values are initialized with d(-1) = 1. The DBPSK constellation is shown in the Appendix F.

### 2.2.4 Spread Spectrum

The figure of merit is the processing gain represented by the number of chips available in the sequence to perform the slicing in small pieces of random polarity, in this project those sequences are the Golay sequences.

In this case, the implementation for spread spectrum is DSSS. An extra operation is included in the standard which is a proportional to $\frac{\pi}{2}$ phase rotation in every chip depending on the position on the chip, consequently, the first symbol would not be rotated, the second $\frac{\pi}{2}$, the third $\pi$, the fourth $\frac{2\pi}{3}$ periodically repeated.

The signal used to implement the DSSS is a Ga32, consequently, the spread spectrum factor would be N = 32. The processing gain introduced by this procedure is shown in the Formula 2.2:

$$G = 10log(N) = 15.05dB \tag{2.2}$$

Consequently, the Control Layer performs properly at -15 SNR lower conditions than other layers.

## 2.3 Single Carrier (SC)

The Single Carrier PHY is implemented to provide low rate throughput. 12 MCS schemes are implemented using different modulation orders and coding rates. The procedure to generate a packet in this PHY is explained.

### 2.3.1 Preamble generation

The preamble is generated using Golay sequences. The preamble is formed appending 17 Ga128 symbols sequences. A Ga128 symbols sequence is repeated 16 times followed by one –Ga128 sequence. As a result, a 2176 symbols sequence is generated. The CE field is formed by 2 different 512 long sequences, Gv512 and Gu512 formed by combinations of Ga128 and Gb128 resulting in an 1152 symbols sequence and a –Gb128 symbols sequence. The preamble structure for SC is shown in Figure 2.4.

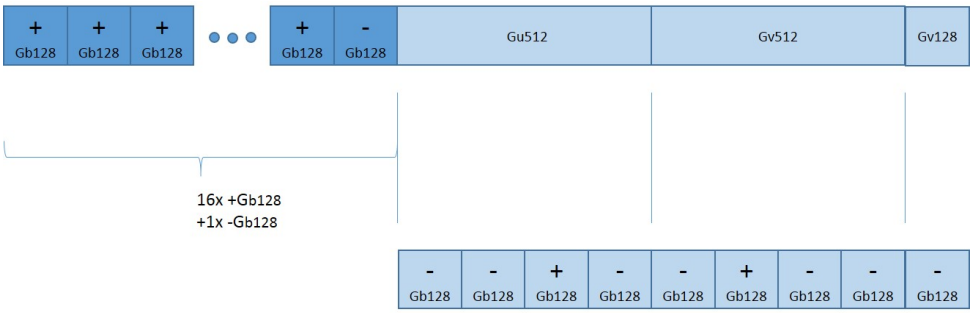


FIGURE 2.4: SC preamble structure.

### 2.3.2 Header encoding

- The header consists of 64 bits. The header structure is shown in the Figure 2.5. There are 14 additional bits considering the Control Layer as a reference, the differences are commented:
  - Scrambler initialization: The scrambler initial state has 7 bits and there is not initial reserved bit, unlike the Control Layer which has 4 bits and initial reserved bit.
  - Length (data): The length field has 18 bits. Therefore, the range is 1 octet to 262143 octets.
  - Last RSSI: This field displays the power level of the last field received.
  - 4 bits (position 45-48) are reserved.

    Another fields for higher layers are implemented such as Additional PPDU, Aggregation, Beam Tracking Request, Turnaround, Last RSSI, and Packet Type.
- Header coding.
  - Scrambling: The 64 bits are scrambled using the initial state set in the header. As it is explained in the Appendix A.1.1.
  - LDPC encoding: The $\frac{3}{4}$ coding rate is used. 672 coded word is fixed, consequently, the input word is 504 long sequence. In order to fulfill a 504 long word, a 440 zero padding is added [1]. As it is explained in the Appendix D.1.1.
  - Sequence fragmentation: The signal is fragmented to replicate the signal in 2 sequences and concatenated in a 448 bit sequence.
    * $c1 = (q_1, q_2, \ldots, q_{LH}, p_1, p_2, \ldots, p_{160})$
    * $c2 = (q_1, q_2, \ldots, q_{LH}, p_1, p_2, \ldots, p_{152}, p_{161}, p_{162}, \ldots, p_{168})$
  - Modulation: The $\frac{\pi}{2}$ - BPSK is used as it is described in 2.3.4.
  - Packetization: The header is packet in 2 block separated by a guard interval. The second resulting symbols sequence it is the same than the first one and multiplied by -1, and then perpended with NGI (Normal Guard Interval) guard symbols. This section is explained in the Appendix C.1.2.

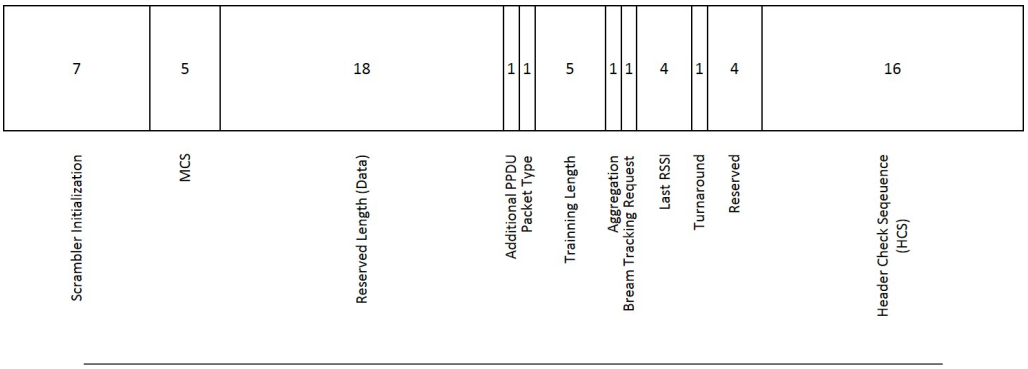


FIGURE 2.5: SC Header structure.

### 2.3.3 Data encoding

- The payload coding follows a similar procedure to encode the header explained in the following steps:
  - Scramble: The scramble procedure is done using the remaining state of the LFSR after the header scrambling. As it is explained in the Appendix A.1.1.
  - LDPC encoding: 4 different coding rates are used in different modes ($\frac{1}{2}$, $\frac{5}{8}$, $\frac{3}{4}$, $\frac{13}{16}$). The codewords are fixed to 672 bits coded length word independently of the code rate, consequently, the input word is fixed depending of the size of the parity matrix and the number of octets fixed in the header. An extra procedure is included in coding in MCS 1. MCS 1 is coded stronger and the modulation order is the lowest available [1]. As a consequence, it is a mode which is more robust in noise environments. In the encoding part this aspect is considered (coding scheme rate is $\frac{1}{2}$) and the input size is 168 instead of 336 length sequence, and zero padded until fulfill 336 bits sequence. After encoding, 336 data bits are xored with LFSR scrambling state. This section is explained in the Appendix C.1.2.
  - Modulation: The modulation scheme is used depending on the MCS used, as it is explained in 2.3.4.
  - Packetization: Each group of NCBPB (NCBPS is shown in the Table D.1) bits is pre-pended by $\frac{\pi}{2} - BPSK$ symbols generated by the 64 point Golay sequence Ga64. The starting index for the first symbol for $\frac{\pi}{2}$ rotation is 0.

### 2.3.4 Modulation mapping

#### $\frac{\pi}{2}$ - BPSK Modulation

The input bit stream is mapped in 2 bits and mapped according to the following equation:

$$s_k = 2c_k - 1 \tag{2.3}$$

The $\frac{\pi}{2}$ - BPSK constellation is shown in Appendix F. A phase rotation procedure is implemented following the Equation 2.4.

$$\hat{s_k} = s_k e^{-j\pi\frac{k}{2}} \tag{2.4}$$

#### $\frac{\pi}{2}$ - QPSK Modulation

The input bit stream is grouped into sets of 2 bits and mapped according to the following equation:

$$s_k = \frac{1}{\sqrt{2}}[(2c_{2k} - 1) - j(2c_{2k+1} - 1)]e^{\frac{-j\pi}{4}} \tag{2.5}$$

The $\frac{\pi}{2}$ - QPSK constellation is shown in Appendix F. A phase rotation procedure is implemented following the Equation 2.4.

#### $\frac{\pi}{2}$ - 16-QAM Modulation

The input bit stream is grouped into sets of 4 bits and mapped according to the following equation:

$$s_k = \frac{1}{\sqrt{10}}[(4c_{4k} - 2) - (2c_{4k} - 1)(2c_{4k+1} - 1) - j(4c_{4k+2} - 2) - (2c_{4k+2} - 1)(2c_{4k+3} - 1)] \tag{2.6}$$

The $\frac{\pi}{2}$ - 16-QAM constellation is shown in F. A phase rotation procedure is implemented following the Equation 2.4.

## 2.4 Low Power Single Carrier (LPSC)

The Low Power Single Carrier PHY is implemented to provide low rate throughput with low power consumption encoders. 7 MCS schemes are implemented using different modulation orders and coding rates. The procedure to generate a packet in this PHY is explained.

### 2.4.1 Preamble generation

The preamble structure is equal to the SC preamble structure shown in Figure 2.5.

### 2.4.2 Header encoding

- Header bits generation: The header bit structure is equal to the SC PHY.
  - Scrambling: The 64 bits are scrambled using the initial state set in the header. As it is explained in the Appendix A.1.1.
  - Reed Solomon encoding: The 64 bits are fragmented in 8 bits and a Reed-Solomon (24,8), generating 24 octets [6]. The procedure is explained in Appendix D.2.1.
  - Block code encoding: The (BC) Block Code (16, 8) is used, consequently, the coding rate is $\frac{1}{2}$ generating 48 octet [6]. The procedure is explained in Appendix D.3.1.
  - Interleaving: A 7 octets interleaving is used. In order to fit the input size of the interleaver an octet pad is added. Each set of 7 octets is interleaved using a uniform interleaver of 7 rows and 8 columns. The 7 octets are written row wise and read column wise. In order to accomplish it, the

following formula was used.

$$i = 8(k\text{mod}(7)) + \text{floor}(\frac{k}{7}) \tag{2.7}$$

where k = 1 to 55 and i is the position of the symbol at the output stream of data.

- Packetitation: 49 octets are generated as it is described and $\frac{\pi}{2}$ - BPSK is used. This section is explained in the Appendix C.1.1.

### 2.4.3 Data encoding

- The payload coding follows a similar procedure to encode the header as it it is explained in the following steps:
  - Scramble: The scramble procedure is done using the remaining state of the LFSR after the header scrambling. As it is explained in the Appendix A.1.1.
  - Reed Solomon & Block Code encoding: As the header is encoded, the payload is encoded in two steps. In the first step, a Reed Solomon (224,208) is used in every mode, the payload is divided in fragments of 208 octets, Reed-Solomon coding is done in byte level. In the case that the payload is a not multiple of 208 bytes, the last K block is shorter that 208 bytes, then Reed-Solomon (16+K, K) is used. In the second step, a Block Code (N, 8) is done after Reed-Solomon coding [6]. Block coding is explained in the Appendix D.3.1 and Reed Solomon in the Appendix D.2.1.
  - Interleaving: The coded bits are fragmented in packets of 7 octets and interleaved as it is explained in 2.4.2.
  - Packetitation: The output bit streams are generated as it is described and modulated. This section is explained in the Appendix C.1.1.

## 2.5 Orthogonal Frequency-Division Multiple (OFDM) access

The OFDM PHY is implemented to provide high rate throughput. 12 MCS schemes are implemented using different modulation orders and coding rates. The procedure to generate a packet in this PHY is explained.

### 2.5.1 Preamble generation

The preamble is generated using Golay sequences. The preamble is formed appending 17 Ga128 symbols sequences. A Ga128 symbols sequence is repeated 16 times followed by one –Ga128 symbols sequence. As a result, a 2176 symbols sequence is generated. The CE field is formed by 2 different 512 long sequences, Gv512 and Gu512 formed by combinations of Ga128 and Gb128 resulting in an 1152 long symbols sequence, and a –Gb128. The CE field is equal to the Single Carrier CE field except that the order of the Gv512 and Gu512 sequences are inverted. The preamble structure for OFDM is shown in Figure 2.6.

### 2.5.2 Header encoding

- Header bits generation: The header consists of 64 bits. The header structure is shown in Figure 2.7. Considering the Single Carrier PHY as a reference, the

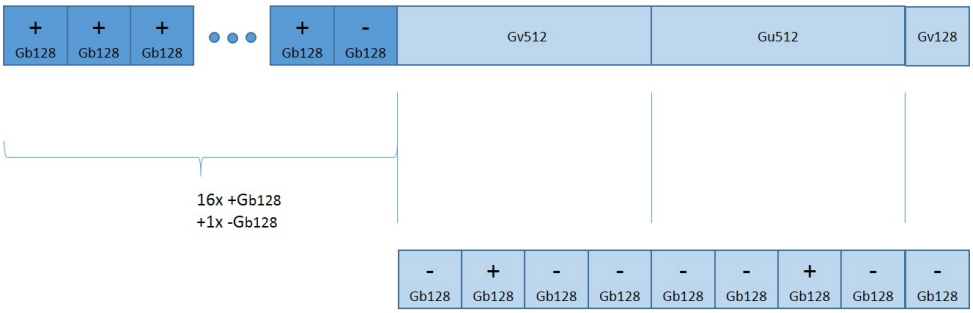


FIGURE 2.6: OFDM preamble structure.

difference is that 2 of the reserved bits of the Singles Carrier PHY are used in the OFDM PHY for the DTP Indicator and the Tone Paring Type. The former fields indicate how to assign the symbols to the subcarriers.

- Header coding.
  - Scrambling: The 64 bits are scrambled using the initial state set in the header. As it is explained in the Appendix A.1.1.
  - LDPC encoding: A $\frac{3}{4}$ coding rate is used. 672 coded word is fixed, consequently, the input word is 504 long sequence. In order to fulfill a 504 long word, a 440 zero padding is added [1].
  - Sequence fragmentation: The signal is fragmented to replicate the signal in 3 sequences and concatenated in a 672 bit sequence. As it is explained in the Appendix D.1.1.
    * $c_1 = (q_1, q_2, \ldots, q_{LH}, p_9, p_{10}, \ldots, p_{168})$.
    * $c_2 = (q_1, q_2, \ldots, q_{LH}, p_1, p_2, \ldots, p_{84}, p_{93}, p_{94}, \ldots, p_{168})$ stored using the scramble state.
    * $c_3 = (q_1, q_2, \ldots, q_{LH}, p_1, p_2, \ldots, p_{160})$ xored using the scramble state.
    * $c = (c_1, c_2, c_3)$
  - OFDM symbol: The QPSK sequences is modulated and IFFT transformed after include the pilot. As it is explained 2.5.5.

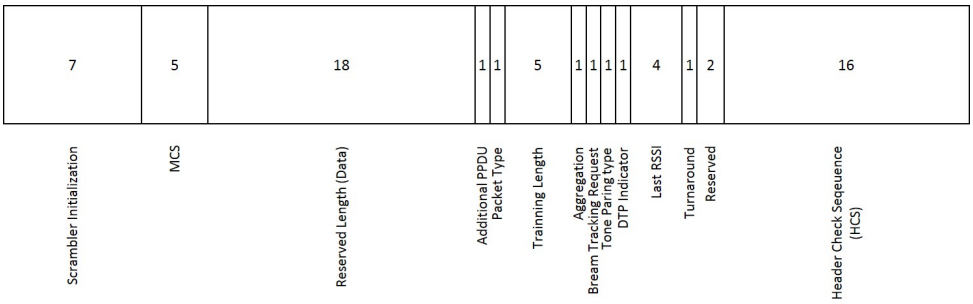


FIGURE 2.7: OFDM Header structure.

### 2.5.3 Data encoding

- The payload coding follows a similar procedure to encode the header as it it is explained in the following steps:
  - Scramble: The scramble procedure is done using the remaining state of the LFSR after the header scrambling. As it is explained in the Appendix A.1.1.
  - LDPC encoding: 4 different coding rates are used in different modes ($\frac{1}{2}$,$\frac{5}{8}$, $\frac{3}{4}$, $\frac{13}{16}$). 672 bits coded length word is fixed independently of the code rate, consequently, the input word is fixed depending of the size of the parity matrix and the number of octets fixed in the header. After padding the word is coding using a specific parity matrix depending on the MCS. As it is explained in the Appendix D.1.1.
  - OFDM symbol: The sequence is modulated depending on the MCS and IFFT transformed after include the pilot. As it is explained in 2.5.4.
  - Clipping: The OFDM waveform is characterized for being a signal whose PAPR is high. Intermodulation products and quantization error could happened if PAPR is not reduced, consequently, it is reduced clipping the signal as it is explained in 2.5.6.

### 2.5.4 Modulation mapping

#### SQPSK Modulation

The SQPSK (Spread Quaternary Phase-Shift Keying) modulation takes the input stream and it is broken into groups of 2 bits. Each pair of bits is converted in a complex constellation of symbols using the formula:

$$d_k^{(q)} = \frac{1}{\sqrt{2}}((2c_{2k}^{(q)} - 1) + j(2c_{2k+1}^{(q)} - 1)) \tag{2.8}$$

This generate a constellation of points for half of the carriers. For the other half of carrier the symbols are the same, nevertheless, the replica is conjugated.

The constellation of the SQPSK modulation is equal to the constellation of the $\frac{\pi}{2}$ - QPSK Modulation constellation shown in the Appendix F.

$$d_{P(k)}^{(q)} = \mathrm{conj}(d_k^{(q)}) \tag{2.9}$$

#### QPSK Modulation

The input stream is broken into groups of 2 bits. Each pair of bits is converted in a complex constellation of symbols using the formula:

$$x_{2k}^{(q)} = \frac{1}{\sqrt{2}}((2c_{4k}^{(q)} - 1) + j(2c_{4k+2}^{(q)} - 1)) \tag{2.10}$$

$$x_{2k}^{(q)} = \frac{1}{\sqrt{2}}((2c_{4k+1}^{(q)} - 1) + j(2c_{4k+4}^{(q)} - 1)) \tag{2.11}$$

$$[d_k^q, d_{P(k)}^q]^T = Q[x_{2k}^q, x_{2k+1}^q]^T \tag{2.12}$$

$$Q = \frac{1}{\sqrt{5}} \begin{pmatrix} 1 & 2 \\ -2 & 1 \end{pmatrix} \tag{2.13}$$

The constellation of the QPSK Modulation is equal to the the constellation of the $\frac{\pi}{2}$ - QPSK modulation constellation shown in the Appendix F.

#### 16-QAM Modulation

The input stream is broken into groups of 4 bits. Each pair of bits is converted in a complex constellation of symbols using the formula:

$$\begin{aligned} x_{2k}^{(q)} = \frac{1}{\sqrt{10}}[(4c_{4k}^{(q)} - 2) - (2c_{4k}^{(q)} - 1)(2c_{4k+1}^{(q)} - 1)]) \\ + j[(4c_{4k+2}^{(q)} - 2) - (2c_{4k+2}^{(q)} - 1)(2c_{4k+3}^{(q)} - 1)] \end{aligned} \tag{2.14}$$

$$\begin{aligned} x_{2k}^{(q)} = \frac{1}{\sqrt{10}}[(4c_{4k+2N_{SD}}^{(q)} - 2) - (2c_{4k+2N_{SD}}^{(q)} - 1)(2c_{4k+1+2N_{SD}}^{(q)} - 1)]) \\ + j[(4c_{4k+2+2N_{SD}}^{(q)} - 2) - (2c_{4k+2+2N_{SD}}^{(q)} - 1)(2c_{4k+3+2N_{SD}}^{(q)} - 1)] \end{aligned} \tag{2.15}$$

The 16-QAM constellation is equal to the $\frac{\pi}{2}$ - 16-QAM constellation. It is shown in Figure F.3.

#### 64-QAM Modulation

The input stream is broken into groups of 6 bits. Each pair of bits is converted in a complex constellation, shown in the Appendix F, of symbols using the formula:

$$\begin{aligned} x_{2k}^{(q)} = \frac{1}{\sqrt{42}}[(8c_{6m}^{(q)} - 4) - (4c_{6m}^{(q)} - 1)(4c_{6m+1}^{(q)} - 2) + (2c_{6m}^{(q)} - 1)(2c_{6m+2}^{(q)} - 1)(2c_{6m+2}^{(q)} - 1)] \\ +j[(8c_{6m+3}^{(q)} - 4) - (4c_{6m+3}^{(q)} - 1)(4c_{6m+4}^{(q)} - 2) + (2c_{6m+3}^{(q)} - 1)(2c_{6m+4}^{(q)} - 1)(2c_{6m+5}^{(q)} - 1)] \\ m = 112(k \bmod (3)) + (\frac{k}{3}), k = 0, 1, \ldots, N_{SD} - 1 \end{aligned} \tag{2.16}$$

### 2.5.5 OFDM symbol

The OFDM symbol conversation is the procedure to spread the information a long several carriers with lower bitrate in order to improve the behaviour of the system against a multipath environment. Fading does not affect to the totality of the carriers, consequently, the information can be recovered. The pilots and data assignment per carrier are shown in the Tables 2.1 and 2.2.

The standard fixes the number of subcarrier to 336. Moreover, DC carriers are included. OFDM modulation is accomplished with a $512N_{UP}$ size including $128N_{UP}$ as a cyclic prefix. Therefore, the FFT size is $640N_{UP}$, where $N_{UP}$ is the up sampling factor.

TABLE 2.1: Pilot subcarrier location

| P(k) | Values |
|---|---|
| -150 | -1 |
| -130 | +1 |
| -110 | -1 |
| -90 | +1 |
| -70 | +1 |
| -50 | -1 |
| -30 | -1 |
| -10 | -1 |
| +10 | -1 |
| +30 | -1 |
| +50 | +1 |
| +70 | +1 |
| +90 | +1 |
| +110 | -1 |
| +130 | +1 |
| +150 | +1 |

TABLE 2.2: Data subcarrier location

| M(k) | Values |
|---|---|
| k + 178 | $-177 \leq k \leq -151$ |
| k + 177 | $-149 \leq k \leq -131$ |
| k + 176 | $-129 \leq k \leq -111$ |
| k + 175 | $-109 \leq k \leq -91$ |
| k + 174 | $-89 \leq k \leq -71$ |
| k + 173 | $-69 \leq k \leq -51$ |
| k + 172 | $-49 \leq k \leq -31$ |
| k + 171 | $-29 \leq k \leq -11$ |
| k + 170 | $-9 \leq k \leq -2$ |
| k + 167 | $2 \leq k \leq 9$ |
| k + 166 | $11 \leq k \leq 29$ |
| k + 165 | $31 \leq k \leq 49$ |
| k + 164 | $51 \leq k \leq 69$ |
| k + 163 | $71 \leq k \leq 89$ |
| k + 162 | $91 \leq k \leq 109$ |
| k + 161 | $111 \leq k \leq 129$ |
| k + 160 | $131 \leq k \leq 149$ |
| k + 159 | $151 \leq k \leq 177$ |

### 2.5.6 Technique to reduced PAPR in OFDM

The ODFM signals are peaky. This phenomenon could affect the quality of the transmission procedure especially in two aspects, quantization and power amplification.

The DAC quantization procedure introduces an quantization error due to the resolution. Assigning a value to a continuous wave signal could not be as accurate as it is needed, in this project the resolution of the signal is double, however, the quantization is limited by the hardware used, therefore, it is done by 8 bits DAC. Peaks concentrate a meaningful part of the energy in low time ranges, losing resolution in this peaks could mean variating the average energy of the signal changing the waveform. Hence, errors are introduced.

The power amplifier could degrade the quality of the transmission due to the non-linear effects which could be introduced. The power amplifier runs in a specific work point which represents an average power input value. Therefore, meaningful differences between peaks and average power could introduce a power higher than the 1 dB compression point. Hence, distorting the signal introducing frequency components.

Signal distortion techniques are intended to reduce peaks amplitudes by non-linear effects. Some of those techniques are clipping and peak windowing or soft clipping.

Clipping is a multiplication of OFDM signal by a window with amplitude equal to 1 if the signal is not clipped and smaller than 1 if the signal is clipped.

Additionally, another problem which clipping generates is frequency distortion. Windowing procedure is used to limit the power peaks, consequently, transitions are introduced. Nevertheless, different type of windows are used in order to mitigate this phenomenon.

The clipping procedure is applied using 2 types of window. The first one is a rectangular window and the second one is an arctangent window. The rectangular window is characterized for being hard clipping, a maximum value is detected and only a specific percentage of instantaneous energy is considered. If any other peaks are detected, they are limited to that energy percentage. The spectral properties and performance are worse than the arctangent window properties, however, the complexity is lower, since it is used to obtain a first approximation about the BER curve degradation.

Rectangular window: A first approach with rectangular windows is done using 3 different thresholds. These levels are percentages of the maximum value of the signal to differentiate the peaks and the majority of the signal energy. This 3 values are 1, 0.85, and 0.75. The first one considered the 100% of the energy, 0.85 and 0.75 includes the energy of the signal under the 85% and 75% of the maximum instantaneous energy.

Arctangent window: The out-of band emission can be reduced by peak windowing, which is clipping plus smoothing to improve spectral properties. Arctangent

windows introduce a smooth transition in the peaks, improving the spectral distortion. However, the relationship between the input and the output of the window in the low energy values could be distorted.

Window function transition is represented by the following equation, where c is a correction term for lineal distortion.

$$w(x) = c\tan^{-1}(\frac{x}{c}) \tag{2.17}$$

As it is commented 3 clipp levels (1, 0.85, 0.75) were tested. The simulations with the former values are shown in Figure 2.8.

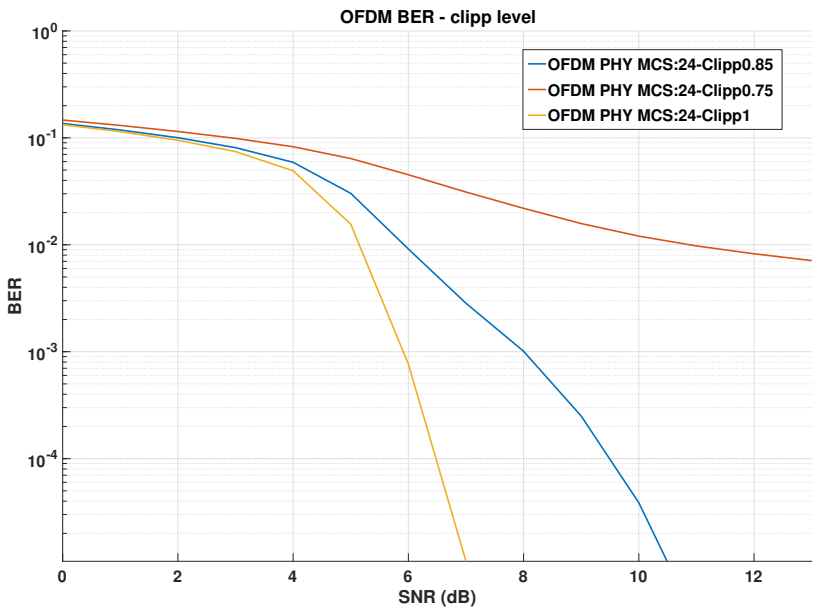


FIGURE 2.8: OFDM clipping simulations (arcustangens window).

To conclude Chapter 2, it can be observed that the main objective of the transmitter is to generate data packets following a specific structure depending on the PHY used. These four PHYs are Control Layer, Single Carrier, Low Power Single Carrier, and OFDM. Each packet of data is coded and modulated differently depending on the PHY and the MCS, but the general structure is Scrambling + Coding + Modulation + Packet + Upsampling + Filtering. There are 4 different modulation orders, 4 coding rates for LDPC, and 5 coding rates for the combination of Reed Solomon and Block coding.

# Chapter 3

# Receiver

The project copes with two different scenarios considering that the vehicles are equipped or not with 802.11ad devices. Signal detection works equally in both cases. However, ranging application uses the reflected waveform in the only one car equipped case and the transmitted and the received waveform in the multiple cars equipped case. Data transmission is also different since it is disabled in the one car case. The Figure 3.1 represents the receiver scheme for each application.

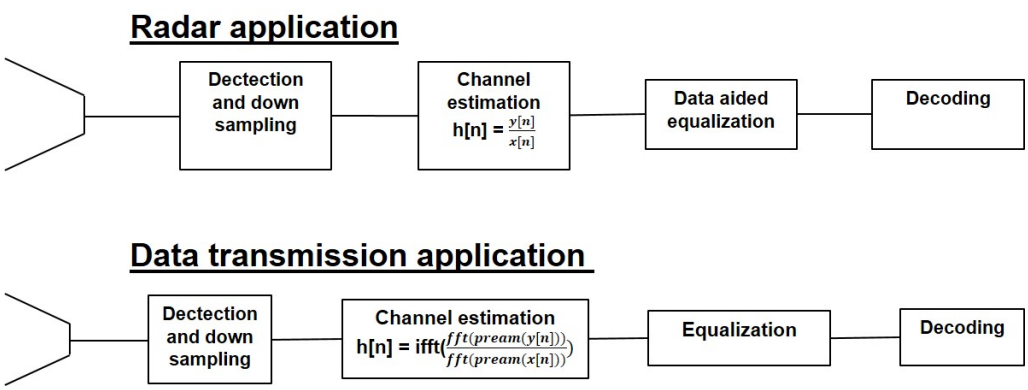


FIGURE 3.1: Applications scheme.

## 3.1 Signal detection & ranging

The signal detection part is focused on the user case which describes a vehicle which is equipped with the necessary equipment to implement 802.11ad functionalities unlike surrounding vehicles. The signal reflected at surfaces in the not equipped vehicle is received by the equipped car and the delay is calculated to infer the position of the not equipped car. The results obtained and the Neyman-Pearson detection theory to obtain the results are explained in the section 4.2.1.

### 3.1.1 Payload autocorrelation vs preamble autocorrelation

Golay sequences present excellent autocorrelation properties for detection since the autocorrelation function of a Golay sequence is the Dirac delta scaled by the length of the sequence.

The autocorrelation properties of the sequences improve increasing the length of the signal. However, the main issue is finding sequences long enough which keep

these properties.

Another type of signal which has similar autocorrelation properties are signal which have a white noise distribution. In other words, the following symbols are unpredictable.

The Figure 4.5 at the left side shows the payload autocorrelation of 8000 symbols. It is also observed in the Figure 4.6 at the left side the autocorrelation of the preamble. The preamble is formed appending different Ga128 and Gb128 as it is observed in the Figure 2.6 for OFDM and a similar structure in the Figure 4.5 for SC. For high SNR values the performance of the system is equal for high and false alarm probability values . However, for lower SNR and lower false alarm probability values the performance of the system is better for the payload detection case than for the preamble detection case. It is observed in the Figure 4.6 and in the Figure 4.5 at the right side.

The correlation between transmitted and received signal is accomplished and a peak is obtained if the signals are aligned considering the transmission delays. However, every 128 delay units a peak is obtained due to the entire preamble is formed by 128 length subsequences whose autocorrelation function is a Dirac delta when those subsequences are aligned, this phenomenon is observed in the Figure 4.5. Obtaining several peaks the system resolution is limited because it is not able to differentiate if the peaks are ghost targets or Ga128/Gb128 autocorrelation peaks. As a consequence, the system is not able to distinguish targets which have a difference in time lower than 1.89 $\mu s$ using the preamble. The calculus are done with the following formula:

$$3328T_{SC} = 4992T_{OFDM} = 1.89\mu s \tag{3.1}$$

The structure of the PDDUs is formed by a preamble and header+payload. The payload structure is considered as a white stochastic process. Hence, its autocorrelation function is a Dirac delta which presents a good performance for detection. The length of payload is fixed for testing at 1023 octets, therefore, the length of the payload is the longest part of the packet in every MCS, and then it is the part used for detection.

Considering the preamble + payload for the detection could be a better option due to the entire sequence is longer than the preamble and both are known at the receiver and the transmitter. However, it must be considered that the preamble is formed by Gu512 sequences which is formed by Ga128 and Gb128 sequences. Hence, the correlations peaks would occur not only when the signals are aligned, it would occur also in 128 units shifts generating several peaks which could conclude in the increment in false alarm detection cases when the signal is considered short as it is in a 1023 octets long payload. The signal could be considered short if the preamble forms the 10% of the entire signal. In the Figure 4.5 at the left side, it can be observed the peaks generated in the autocorrelation function of the preamble.

### 3.1.2 Delay calculation

Autocorrelation is the correlation of a signal with a delayed copy of itself as a function of delay. Consequently, the mayor similarity would be observed when the signal is received and the autocorrelation function would show a peak with a delay which is the transmission time of the signal.

The propagation speed of the signal is $c_0$. Calculating half of the time between the reflectance surface and the location of the other vehicles and considering the signal propagation speed the position is inferred.

$$e = \frac{v \cdot t}{2} \tag{3.2}$$

## 3.2 Signal decoding

Signal decoding is necessary in order to extract the payload information stored in packets. After the detection part, it can be supposed that the PHY of the signal is known since the receiver has information about what signal are sent by the transmitter (radar application), consequently, PHY is chosen.

The information related with signal MCS is stored in the header. This header is coded uniquely depending on the MCS. This information is used by the receiver in order to decode the header received. After header decoding, receiver is able to know 4 fields which are used in the PHY to decode the signal: MCS, initial scramble state, payload length, and HCS.

The MCS decoded is compared with the MCS transmitted and checksum of the received packet is generated with the received decoded header, if the comparison of the checksum with the HCS decoded is positive, the header can be validated and the payload could be decoded. However, if one of the comparison is not positive the packet is discarded.

The packet is valid due to header positive checking and the decoder is initialized with the length value which is stored in the header, it is used to know the quantity of words which must be decoded or the padding among the information.

The payload is decoded and compared with the signal sent quantizing the different values between them in order to check if the signal is well received.

### 3.2.1 Control layer (CL)

The decoding procedure must consider the same procedures implemented in the transmitted part. Nevertheless, those procedures are implemented in the receiver in the inverse order and they must undo the procedures form the transmission part. In Control Layer case the following steps are considered.

- Filtering: As it is established in 802.11ad a spectrum mask requirements must be fulfill. Consequently, a RRC filter is applied in order the smooth the signal transition between symbols. In order to ensure that the ISI is reduced the signal is filtered again at the receiver by a root rise cosine. It is explained in Appendix E.1.2.

- Despreading: The spreading procedure is accomplished in order to add gain codification to improve its performance. Firstly, phase rotation is compensated depending on the position of the symbol rotated. Symbols rotated are multiplied by Ga32 sequence and averaged by the length of the chip sequence. This section is explained in Appendix A.1.2.
- DBPSK demodulation: Differential demodulation is used. The demodulation procedure is accomplished through LLR as it is explained in Appendix A.2.
- LDPC decoding: The $\frac{1}{2}$ coding rate decoding is used as it is explained in Appendix D.1.2.
- Descrambling: The descramble procedure is done using the initial state decoded in the received header. Explained in Appendix A.1.2.
- Header & payload slots union.

### Demodulation mapping

**DBPSK** : Differential demodulation is based on transition between 0 and 1. Consequently, signs of successive likehood ratios are compared. If the signs are equal the likehood ratio is positive. However, if the signs are not equal the likehood ratio is negative.

After differential decoding, BPSK demodulation procedure is used. The expression for the LLR is shown:

$$\text{LLR} = \log_{10}\left(e^{\frac{-|(y-1|^2}{\sigma^2}}\right) - \log_{10}\left(e^{\frac{-|(y-(-1)|^2}{\sigma^2}}\right) \tag{3.3}$$

$$\text{LLR} = \frac{|y-1|^2 - |y-(-1)|^2}{\sigma} \tag{3.4}$$

### Metrics and constellation

In the Figure 3.2 the EVM (error Vector Magnitude) for the MCS 0 graphs is shown. It can be concluded that the requirements are accomplished for low SNR conditions, therefore, for hight SNR conditions in can be assumed that the CL is modulated correctly. The EVM formula for CL PHY is shown. Where $P_{AVG}$ is shown in the Appendix B.4.

$$\text{EVM} = 20\log_{10}\left(\sqrt{\frac{1}{N_s P_{avg}}\sum_{i=1}^{N_S}[(I_i - I_i^*)^2 + (Q_i - Q_i^*)^2]}\right) \tag{3.5}$$

In order to compare the metrics in the lowest and in the highest SNRs, the Figure 3.4 shows the comparison in metrics for the CL PHYs. The metrics section is explained in the Appendix C.

As it can be observed in the Figures 3.3, the SNR = -15 the constellation shows two clusters of data. However, those clusters are overlapped and the BER conditions at this level are worse than at 0 dB (represented in the Figure 3.4), where the cluster are clearly differentiate, as it would be observed in the simulation section.

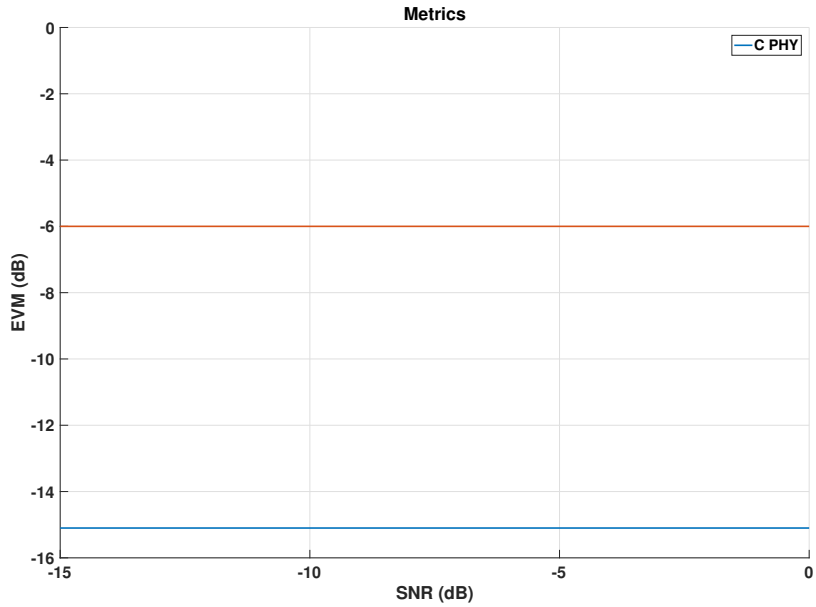


FIGURE 3.2: EVM CL.

### 3.2.2 Single Carrier (SC)

The decoding procedure must consider the same procedures implemented in the transmitted part. Nevertheless, those procedures are implemented in the receiver in the inverse order and they must undo the procedures form the transmission part. In Single Carrier layer case the following steps are considered.

- Header decoding
  - Depacketitation: The header is accomplished in 2 packets of 448 bits and second packets inverted.
  - Demodulation: The BPSK demodulation and phase rotation are done as it is explained in Appendix A.2.
  - Sequence union: Two data slots are combined. The combination of 2 data slots are equally combined due to an AWGN is assumed as a channel.
  - LDPC decoding: The header is LDPC decoded and descrambled using the initial scramble state decoded. Explained in the Appendix A.2.
  - Descrambling: The descramble procedure is done using the initial state decoded in the received header. Explained in Appendix A.2.
- Payload decoding
  - Depacketitation: The guard sequences are discarded to get the coded data.
  - Demodulation: The demodulation procedure is done depending on the MCS detected in header. Demodulators available are: BPSK, $\frac{\pi}{2}$ - QPSK, and $\frac{\pi}{2}$ - 16-QAM. Explained in the Appendix A.2.
  - Descramble: The first descrambler procedure is initiated. Scramble state obtained after header scrambler is not valid in this step. In the transmitter

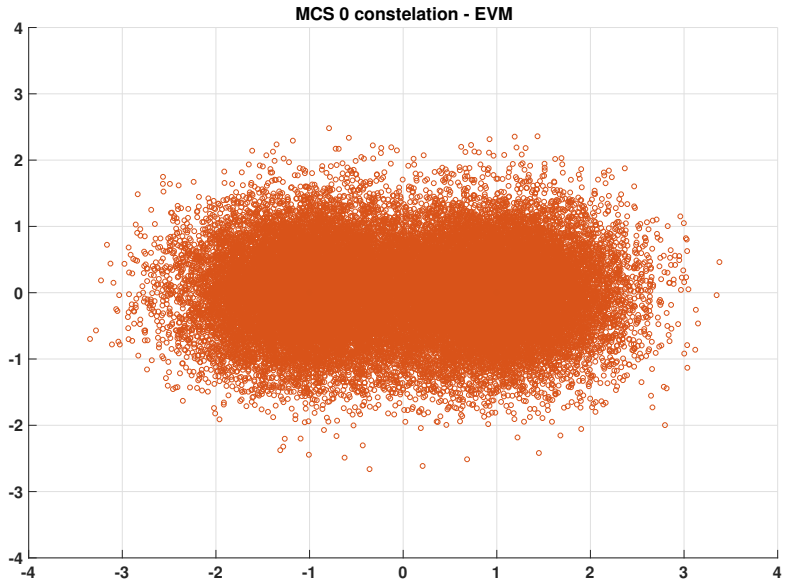


FIGURE 3.3: EVM CL -15 dB.

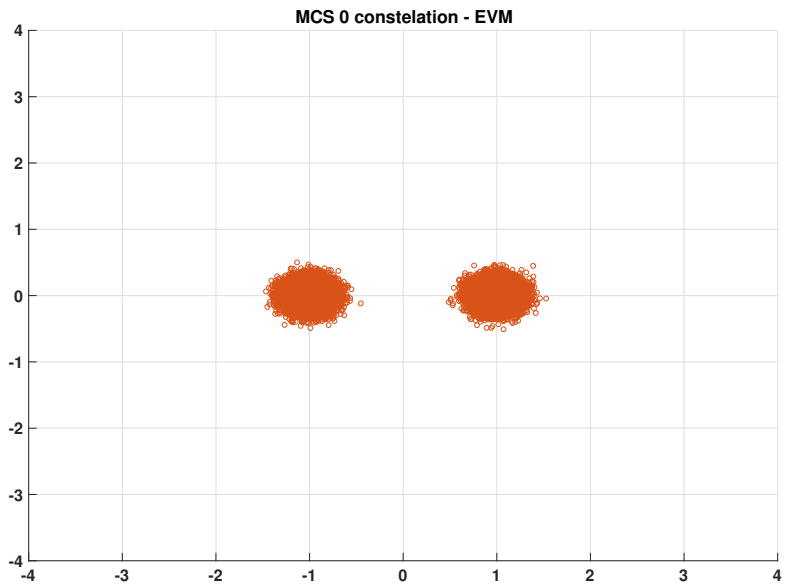


FIGURE 3.4: EVM CL 0 dB.

the scrambler state after header scrambler is used in the first scrambler procedure which is equivalent to the second descrambler in the receiver. Consequently, the state used in the second scrambler in the transmitter is emulated to the first descrambler in the receiver using the header state. Explained in Appendix A.1.2 and a scheme of the procedure is shown in the Figure 3.5.

- LDPC decoding: LDPC decoding is performed depending on the MCS, MCS 1 as an extra procedure which must be consider, this procedure is not done in the MCS 1-12. MCS 1 extra procedure which decreases 25% the time efficiency of the symbol. However, the robustness of the information is increased. The information is not segmented in 336 length sequences, it is divided in 168 bits and the 336 symbols are fulfilled with a replica of the data, but xored. Consequently, the second part of the codeword is xored and averaged with the first 168 sequence bits. The procedure is explained in Appendix A.2.
- Descramble: The second descrambling, which is equivalent with the first scrambling procedure in the transmitter, uses the scramble state form the header. Explained in Appendix A.1.2.

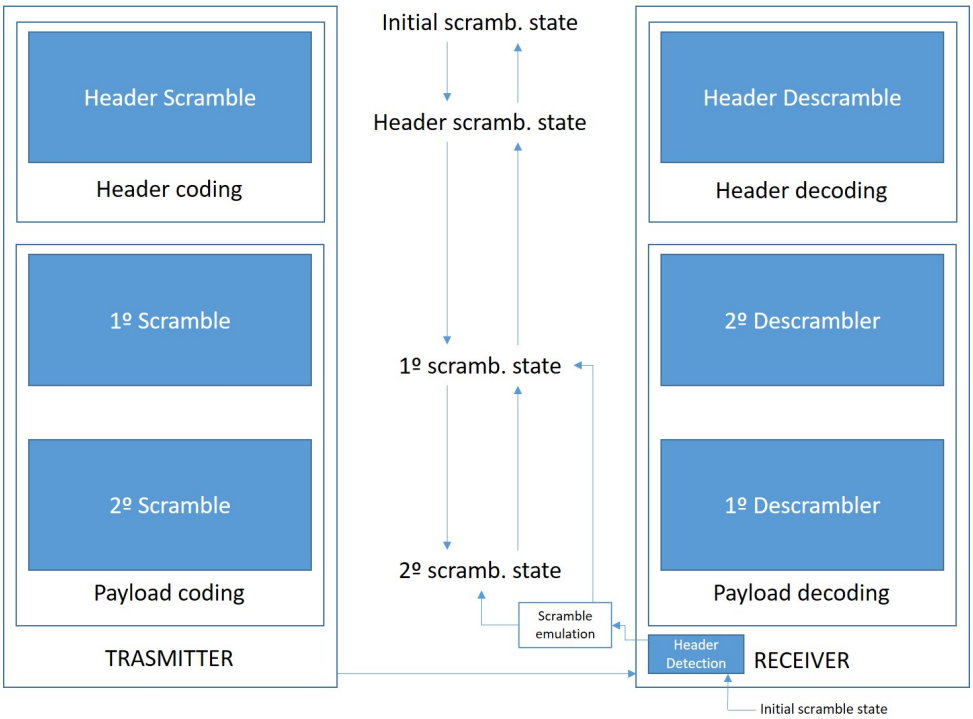


FIGURE 3.5: Descramble Scheme.

### Demodulation mapping

**$\frac{\pi}{2}$ - BPSK Demodulation** : The BPSK modulation compensates the rotation phase performed per symbol and the normalization in amplitude. BPSK is a 1 order modulation, consequently, 1 LLR are considered, one per bit.

The expression for the is shown:

$$\text{LLR} = \frac{|y-(1)|^2 - |y-(-1)|^2}{\sigma} \tag{3.6}$$

**$\frac{\pi}{2}$ - QPSK Demodulation** : The QPSK modulation compensates the rotation phase performed per symbol and the normalization in amplitude. QPSK is a 2 order modulation, consequently, two LLR are considered, one per bit. Average value consider per symbol are $[-\frac{1}{\sqrt{2}}, \frac{1}{\sqrt{2}}]$

$$\text{diff}(1x) = \text{Re}(x) \pm \frac{1}{\sqrt{2}} \tag{3.7}$$

$$\text{diff}(2x) = \text{Imag}(x) \pm \frac{1}{\sqrt{2}} \tag{3.8}$$

Where x = 0,1. The expressions for the 2 LLR are shown:

$$\text{LL1} = \frac{\min(|\text{diff}(11)|) - \min(|\text{diff}(10)|)}{\sigma} \tag{3.9}$$

$$\text{LL2} = \frac{\min(|\text{diff}(21)|) - \min(|\text{diff}(20)|)}{\sigma} \tag{3.10}$$

**$\frac{\pi}{2}$ 16-QAM Demodulation** : The 16-QAM modulation compensates the rotation phase performed per symbol and the normalization in amplitude. 16-QAM is a 4 order modulation, consequently, four LLR are considered, one per bit. Average value consider per symbol are $[\frac{-1}{\sqrt{10}}, \frac{-3}{\sqrt{10}}, \frac{1}{\sqrt{10}}, \frac{3}{\sqrt{10}}]$

$$\text{diff}(xy) = \text{Re}(y) \pm \frac{z}{\sqrt{10}} \tag{3.11}$$

$$\text{diff}(wy) = \text{Imag}(y) \pm \frac{z}{\sqrt{10}} \tag{3.12}$$

Where x = 1,2, w= 4,5, y = 0,1, and z = 1,3. The expressions for the 4 LLR are shown:

$$\text{LL1} = \frac{\min(|\text{diff}(11)|^2) - \min(|\text{diff}(10)|^2)}{\sigma} \tag{3.13}$$

$$\text{LL2} = \frac{\min(|\text{diff}(21)|^2) - \min(|\text{diff}(20)|^2)}{\sigma} \tag{3.14}$$

$$\text{LL3} = \frac{\min(|\text{diff}(31)|^2) - \min(|\text{diff}(30)|^2)}{\sigma} \tag{3.15}$$

$$\text{LL4} = \frac{\min(|\text{diff}(41)|^2) - \min(|\text{diff}(40)|^2)}{\sigma} \tag{3.16}$$

### Metrics and constellation

In the Figure 3.6 the EVM graphs for the MCS 12 is shown. It can be concluded that the requirements are accomplished for high SNR conditions, but it is not fulfilled for low SNR ratio. As it was commented the SNR in the transmitter could be considered high. Consequently, the SC is modulated correctly. The EVM formula for SC PHY is shown. Where $P_{AVG}$ is shown in the Appendix B.4.

$$\text{EVM} = 20\log_{10}\left(\sqrt{\frac{1}{N_s P_{avg}}\sum_{i=1}^{N_S}[(I_i - I_i^* - I_0)^2 + (Q_i - Q_i^* - I_0)^2]}\right) \tag{3.17}$$

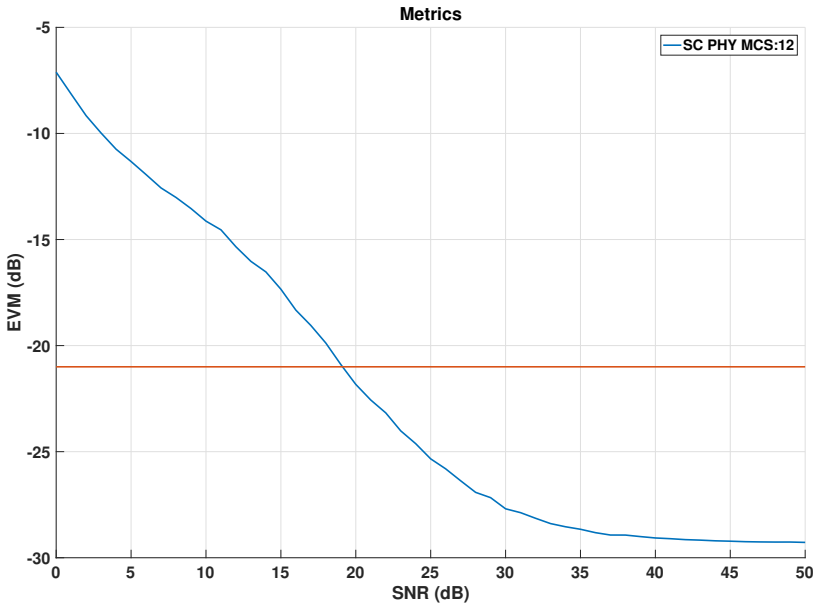


FIGURE 3.6: EVM SC.

In order to compare the metrics in the lowest and in the highest SNRs, the Figure 3.7 shows the constellation when the SNR is 0 dB and the Figure 3.8 in 50 dB conditions. The constellation for 0 dB shown symbols which does not show a 4 bits constellation as it is observed in the 50 dB conditions, for 0 dB SNR the missed packets rate is superior to the 30% and the BER 50% (the receiver is guessing the data stream) as it will be observed in the simulation section. The metrics section is explained in the Appendix C.

### 3.2.3 Low Power Single Carrier (LPSC)

The decoding procedure must consider the same procedures implemented in the transmitted part. Nevertheless, those procedures are implemented in the receiver in the inverse order and they must undo the procedures form the transmission part. In Low Power Single Carrier PHY case the following steps are considered.

- Header decoding
  - Depacketitation: The extraction of the data removing G8 sequences and Ga64.
  - BPSK demodulation: The BPSK demodulation is used. The demodulation procedure is accomplished through LLR as it is explained in Appendix A.2.

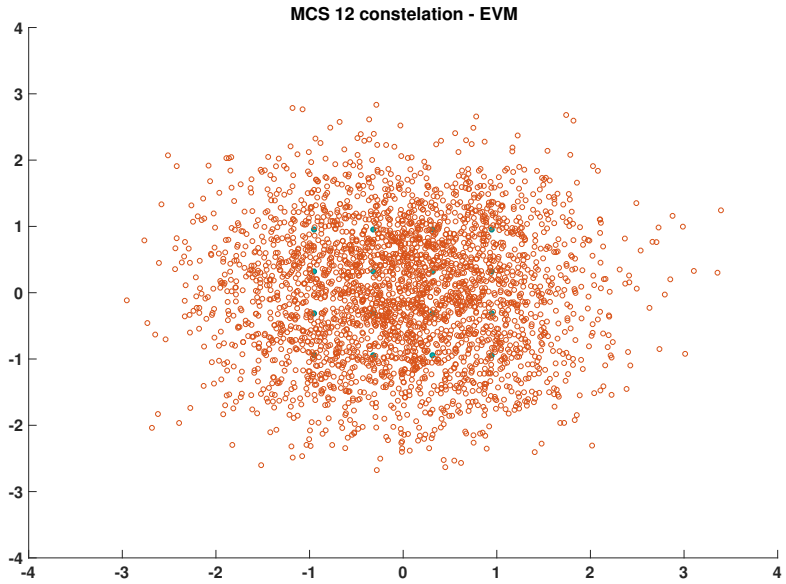


FIGURE 3.7: EVM SC 0 dB.

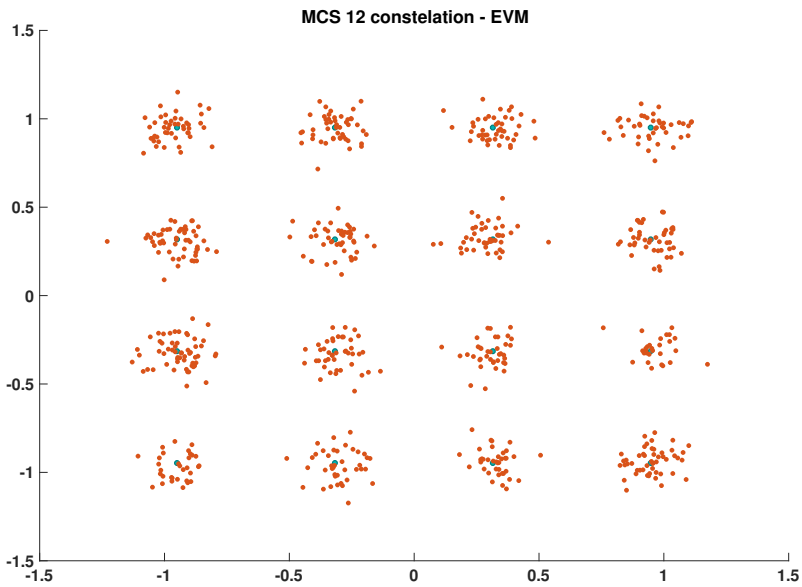


FIGURE 3.8: EVM SC 20 dB.

- Interleaving: The interleaving procedure is used as it is explained in section 3.2.3.
- LLR Hard decision: Transformation from LLR to hard decision. This decision is accomplished in order to reduce the work load of the Reed Solomon decoder even reducing the performance. Hence, the power consumption as is the main objective of the LPSC PHY.
- Reed Solomon decoding: The Reed Solomon decoding is used as it is explained in Appendix D.2.2 [6].
- Block code decoding: The Block Code decoding is used as it is explained in Appendix D.3.2 [6].
- Descrambling: Descrambiling using the scramble state from decoded header. As it is explained in Appendix A.1.2.

• Payload decoding

- Guard Insertion: The extraction of the data removing G8 sequences and Ga64.
- Demodulation: The demodulation procedure is done depending on the MCS detected in header. Demodulators available are: BPSK and $\frac{\pi}{2}$ - QPSK. Procedure explained in Appendix A.2.
- Hard decision: The LLR are transformed to bits to reduce the complexity of the receiver. Hence, the energy consumption as it is the objective of this PHY usage.
- Interleaver: A 7 octets interleaving is used. In order to fit the input size of the interleaver an octet pad is added. Each set of 7 octets is interleaved using a uniform interleaver of 7 rows and 8 columns. The 7 octets are written column wise and read row wise, it is the opposite procedure to the interleaving in the transmitter. In order to accomplish it the following the next formula.

$$8(k\text{mod}(7)) + \text{floor}(\frac{k}{7}) = i \tag{3.18}$$

  where k = 1 to 55 and i the position of the symbol at the output stream of data.
- Descramble: The first descrambler procedure is initiated. Scramble state obtained after header scrambler is not valid in this step. In the transmitter the scrambler state after header scrambler is used in the first scrambler procedure which is equivalent to the second descrambler in the receiver. Consequently, the state used in the second scrambler in the transmitter is emulated to the first descrambler in the receiver using the header state. Explained in Appendix A.1.2 and a scheme of the procedure is shown in the Figure 3.5.
- Block decoding: The Block Code (16,8) decoding procedure is used to generate 24 octets [6]. Explained in Appendix D.3.2.
- Reed Solomon decoding: The Reed-Solomon(24,8) decoding procedure is used to generate 64 bits [6]. Explained in Appendix D.2.2.
- Descramble: The second descrambling, which is equivalent with the first scrambling procedure in the transmitter, uses the scramble stat form the header. As it is explained in Appendix A.1.2.

#### Metrics and constellation

The LPSC mode has not metrics specify, therefore, it is evaluated as a SC in order to observe the constellation for MCS 31 in the highest and in the lowest SNR. The constellation for low SNR conditions is shown in the Figure 3.9 and for high SNR conditions in the Figure 3.10. Where the case of the SC can be also observed in the same conditions, but the modulation order is 2 instead of 4, consequently, the performance is better that the SC as it is explained in the simulations section. The RMS is averaged by the number of the carriers and the average power of the constellation calculated as it is shown in the Appendix B.4.The metrics section is explained in the Appendix C.

### 3.2.4 Orthogonal Frequency-Division Multiple (OFDM) access

The decoding procedure must considers the same procedures implemented in the transmitted part. Nevertheless, those procedures are implemented in the receiver in the inverse order and they must undo the procedures form the transmission part. In OFDM PHY case the following steps are considered.

- Header decoding
  - OFDM symbol demodulation: The ODFM demodulation is accomplished as it is explained in section 3.2.5 and QPSK demodulated as it is explained in sub section 3.2.4.
  - Data union: The data replicated is separated in three data slots. Second slot of data is descrambled and third xored. Three data slots are combined. The 3 data slots are equally combined due to an AWGN is assumed as a channel.
  - LDPC decoded: The header is LDPC decoded and descrambled using the initial scramble state decoded. Explained in the Appendix D.1.2.
  - Descrambling: The descramble procedure is done using the initial state decoded in the received header. As it is explained in Appendix A.1.2.
- Payload decoding
  - OFDM symbol demodulation: The ODFM demodulation is accomplished as it is explained in 3.2.5 and demodulated as it is explained in section 3.2.4. Demodulators available are: SQPSK, QPSK, 16-QAM, and 64-QAM.
  - LDPC decoding: The LDPC decoding is performed depending on the MCS, the procedure is explained in the Appendix D.1.2.
  - Descrambling: The descramble procedure is done using the initial state decoded in the received header. As it is explained in Appendix A.1.2.

#### Demodulation mapping

**SQPSK Demodulation** : The SQPSK modulation compensates the normalization in amplitude. SQPSK is a 2 order modulation, consequently, 2 LLR are considered, one per bit. Moreover, SQPSK considers 2 streams of data, on per group of carriers, since 4 LLR are considered, two per stream.

As QPSK the average values considered are $[-\frac{1}{\sqrt{2}}, \frac{1}{\sqrt{2}}]$ based on the equation of the $\frac{\pi}{2}$ - QPSK of the Single carrier section 3.2.2. The expressions for the 2 LLR are

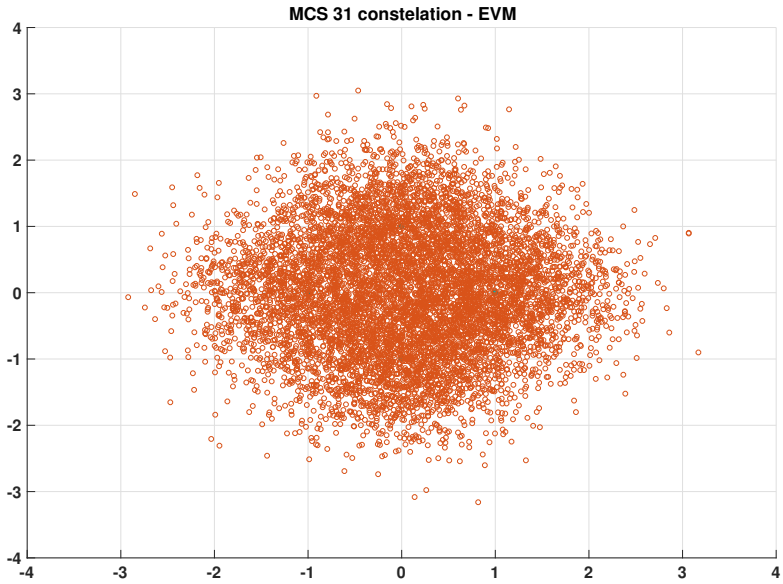


FIGURE 3.9: EVM LPSC 0 dB.

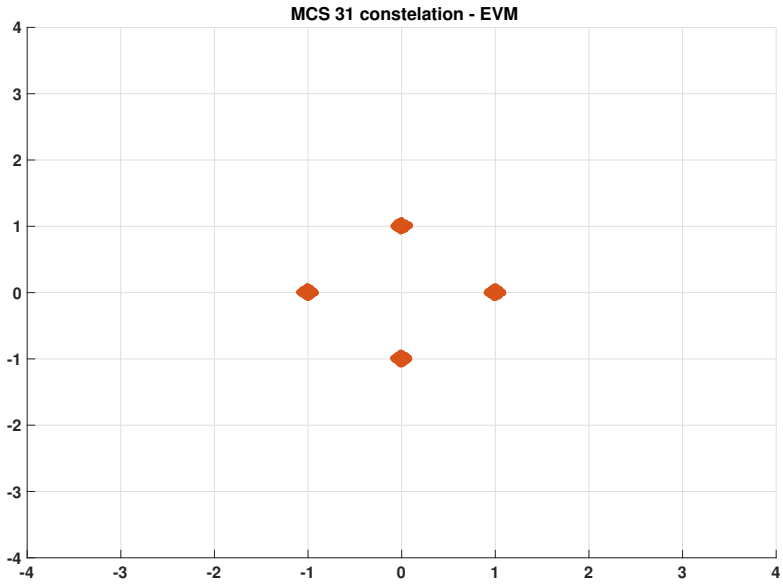


FIGURE 3.10: EVM LPSC 20 dB.

shown, where i = 1,2 streams, not simultaneously.

$$\mathrm{LLR1_i} = \frac{\min(|\mathrm{diff}(11)_i|)^2 - \min(|\mathrm{diff}(10)_i|)^2}{\sigma} \tag{3.19}$$

$$\mathrm{LLR2_i} = \frac{\min(|\mathrm{diff}(21)_i|)^2 - \min(|\mathrm{diff}(20)_i|)^2}{\sigma} \tag{3.20}$$

**QPSK Demodulation** : The QPSK modulation compensates the normalization in amplitude and the transformation of the symbols to equalize both the stream of data in the first group of carrier and the stream of the second group of carriers. QPSK is a 2 order modulation, consequently, 2 LLR are considered, one per bit. Moreover, QPSK considers 2 streams of data, on per group of carriers, since 4 LLR are considered, two per stream.

Average values considered are $[-\frac{1}{\sqrt{2}}, \frac{1}{\sqrt{2}}]$. The LLR equations are the same that the QPSK section equations 3.2.4.

**16-QAM Demodulation** : The 16-QAM modulation compensates the normalization in amplitude. 16-QAM is a 4 order modulation, consequently, 4 LLR are considered, one per bit. Moreover, 16-QAM considers 2 streams of data, on per group of carriers, since 8 LLR are considered, 4 per stream.$[-\frac{1}{\sqrt{(10)}}, -\frac{3}{\sqrt{(10)}}, \frac{1}{\sqrt{(10)}}, \frac{3}{\sqrt{(10)}}]$. The LLR equations are the same that the $\frac{\pi}{2}$ - 16-QAM section equations 3.2.2. The expressions for the 4 LLR are shown, where i = 1,2, not simultaneously.

$$\mathrm{LLR1_i} = \frac{\min(|\mathrm{diff}(11)_i|)^2 - \min(|\mathrm{diff}(10)_i|)^2}{\sigma} \tag{3.21}$$

$$\mathrm{LLR2_i} = \frac{\min(|\mathrm{diff}(21)_i|)^2 - \min(|\mathrm{diff}(20)_i|)^2}{\sigma} \tag{3.22}$$

$$\mathrm{LLR3_i} = \frac{\min(|\mathrm{diff}(31)_i|)^2 - \min(|\mathrm{diff}(30)_i|)^2}{\sigma} \tag{3.23}$$

$$\mathrm{LLR4_i} = \frac{\min(|\mathrm{diff}(41)_i|)^2 - \min(|\mathrm{diff}(40)_i|)^2}{\sigma} \tag{3.24}$$

**64-QAM Demodulation** : The 64-QAM modulation compensates the normalization in amplitude. 64-QAM is a 6 order modulation, consequently, 6 LLR are considered, one per bit. Moreover, 64-QAM considers 3 streams of data, on per group of carriers, since 18 LLR are considered, 6 per stream. Average values considered are $[-\frac{1}{\sqrt{42}}, -\frac{3}{\sqrt{42}}, -\frac{5}{\sqrt{42}}, -\frac{7}{\sqrt{42}}, \frac{1}{\sqrt{42}}, \frac{3}{\sqrt{42}}, \frac{5}{\sqrt{42}}, \frac{7}{\sqrt{42}}]$.

$$\mathrm{diff}(xy)_i = \mathrm{Re}(y) \pm \frac{z}{\sqrt{10}} \tag{3.25}$$

$$\mathrm{diff}(wy)_i = \mathrm{Imag}(y) \pm \frac{z}{\sqrt{10}} \tag{3.26}$$

Where i = 1,2,3 (not simultaneously), x = 1,2,3, w= 4,5,6, y = 0,1, and z = 1,3,5,7. The expressions for the 6 LLR are shown.

$$\mathrm{LLR1_i} = \frac{\min(|\mathrm{diff}11_i|)^2 - \min(|\mathrm{diff}10_i|)^2}{\sigma} \tag{3.27}$$

$$\mathrm{LLR2_i} = \frac{\min(|\mathrm{diff21}_i|)^2 - \min(|\mathrm{diff20}_i|)^2}{\sigma} \tag{3.28}$$

$$\mathrm{LLR3_i} = \frac{\min(|\mathrm{diff31}_i|)^2 - \min(|\mathrm{diff30}_i|)^2}{\sigma} \tag{3.29}$$

$$\mathrm{LLR4_i} = \frac{\min(|\mathrm{diff41}_i|)^2 - \min(|\mathrm{diff40}_i|)^2}{\sigma} \tag{3.30}$$

$$\mathrm{LLR5_i} = \frac{\min(|\mathrm{diff51}_i|)^2 - \min(|\mathrm{diff50}_i|)^2}{\sigma} \tag{3.31}$$

$$\mathrm{LLR6_i} = \frac{\min(|\mathrm{diff61}_i|)^2 - \min(|\mathrm{diff60}_i|)^2}{\sigma} \tag{3.32}$$

### Metrics and constellation

In the Figure 3.11 the EVM graphs is shown. It can be concluded that OFDM modulation is performed correctly due to at high SNR the EVM fulfills the requirements and the constellations shown in the Figure 3.13 shown an expected distribution of the symbols in the constellation either for low and high SNR levels.The EVM formula for OFDM PHY is shown.

$$\mathrm{EVM} = 20\log_{10}\frac{1}{N_f}\sum_{i=1}^{N_f}\sqrt{\frac{\sum_{i=1}^{N_{SYM}}\sum_{k\epsilon K}[(I(i,j,k)-I(i,j,k)^*)^2+(Q(i,j,k)-Q(i,j,k)^*)^2]}{(N_{ST}-N_{DC})N_{SYM}P_0}} \tag{3.33}$$

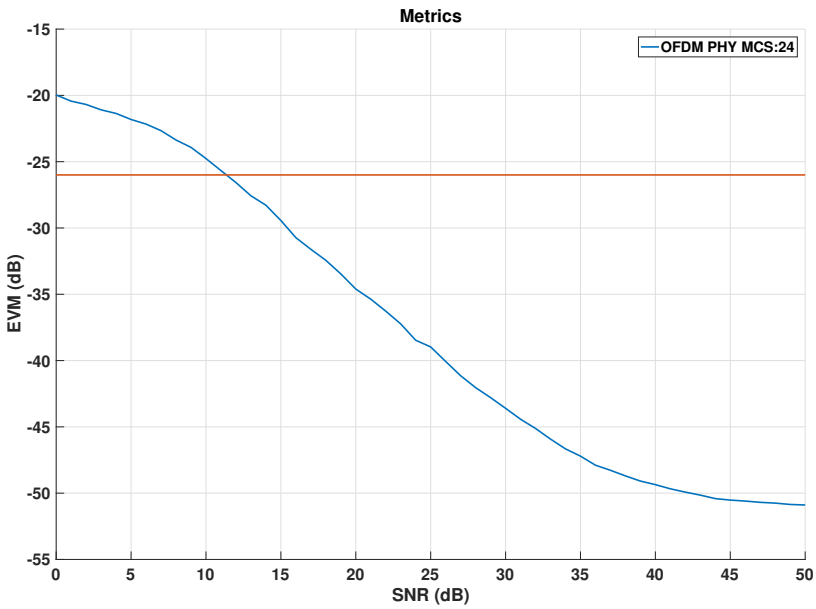


FIGURE 3.11: EVM OFDM.

In order to compare the metrics in the lowest and in the highest SNRs, the Figure 3.12 shows the constellation for low SNR conditions and the Figure 3.13 for high SNR conditions in OFDM PHYs. The metrics section is explained in the Appendix C.

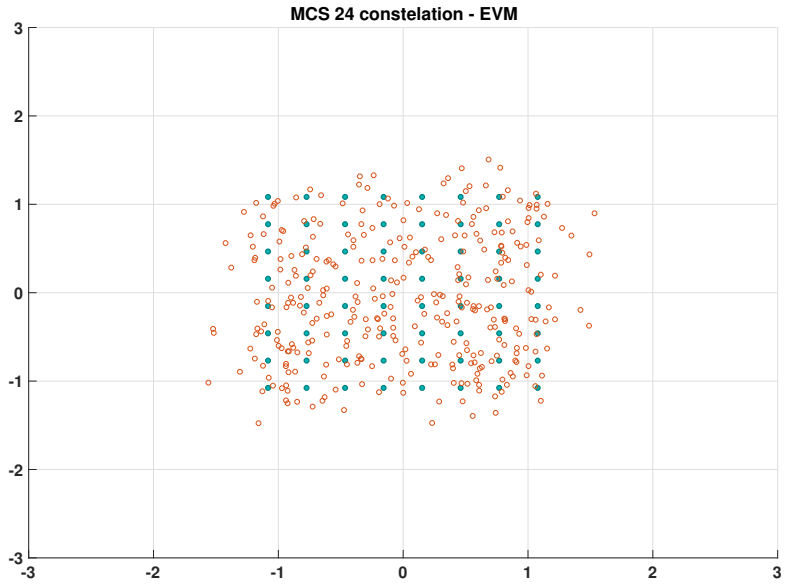


FIGURE 3.12: EVM OFDM 0 dB.

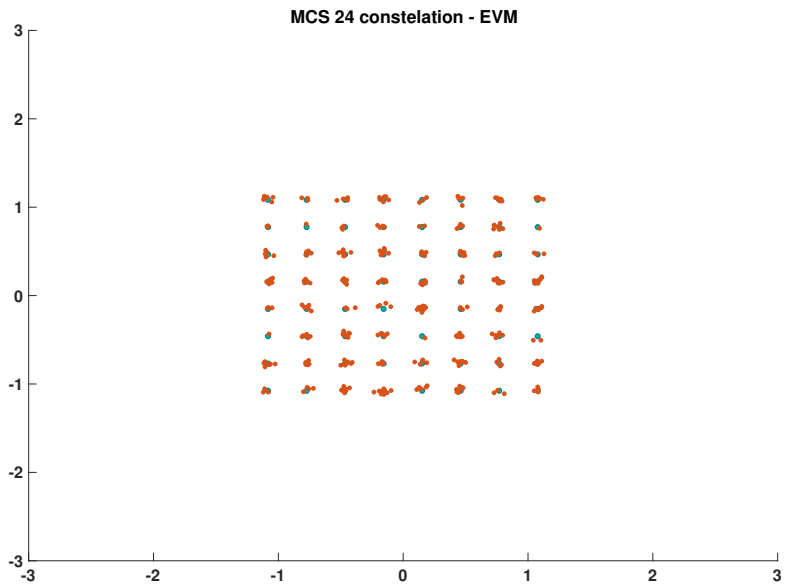


FIGURE 3.13: EVM OFDM 20 dB.

### 3.2.5 OFDM Demodulation

The OFDM demodulation procedure is intended to undo the OFDM modulation procedure, this procedure must be done in every symbol.

Firstly, the cyclic prefix is eliminated and it must be considered if the signal is up sampled. If the signal was up sampled in the transmitter procedure, the size of the IFFT implemented in the transmitter is proportional by the up sampling factor to the number of carriers, consequently, an FFT procedure is accomplished considering the up sampling factor, the amplitude is also denormalized. Secondly, the zero padding done in the transmitter, as a consequence, the up sampling procedure is removed. Finally, the information located in the data carriers is extracted.

In the chapter 3 the receiver is explained. As it is presented in the introduction, there are two applications which are implemented the data transmission and the radar applications.

Data transmission: The procedure explained in the transmitter are undone, the general structures of the receiver is Detection + Downsampling + Depacket + Demodulation + Decoding + Scramble.

Radar application: The procedure is divided in two parts. The detection is accomplished using the entire payload as it is discussed and proved in the section 3.1.1 that the entire signals behaves better than only the preamble to accomplished the detection. Once the peak is detected the delay is calculated.

# Chapter 4

# Simulations

The performance of the system is simulated in order to evaluate the system functionalities. The simulations are accomplished in individual modules and system tests. The individual test are done in order to evaluate that every module performs correctly and system functionalities are evaluated joining every single module evaluated in the individual test to prove the correct performance of the system.

## 4.1 Individual tests

### 4.1.1 Modulator/demodulators

The modulation performance is measured in this section. The modulators are tested using the modulator, the demodulator, the LDPC coder, and the LDPC decoder. The reason to use the LDPC coding scheme is that the output of the modulator is an LLR and that is the input expected by the LDPC decoder. Therefore, to compare bits to generate the error signal for the BER curve a LLR-bits converter is needed, that is the task of the LDPC codification.

The LDPC codification admits 4 different input length depending on the parity matrix, but the output length is fixed to 672 bits, therefore, $\frac{1}{2}$ coding rate is chosen to obtain at the output the longer sequence available, 504 bits, to generate the error signal.

The AWGN signal is added to an input sequence with variable SNR. The number of realization per SNR is set at 1000 and the SNR range of 0 to 18 dB.

The 64-QAM and 16-QAM modulation schemes are exclusively used in OFDM and they require several parallel stream of data. In these cases 3 packets in 64-QAM case and 2 packets in 16-QAM modulations are generated in every realization since several data streams are modulated as the standard requires. The results of the uncoded modulation performance can be observed in the Figure 4.1.

### 4.1.2 Coders

The performance of coder is measured differently depending on the coder used. In the case of LDPC coder its length must be fixed depending on the parity matrix used. However, in Reed Solomon and Block Coding coders the zero padding is adjusted to fulfill the required input lengths.

In the LDPC case one 504 bits input word is used in 100 realizations in a SNR range of -10 to 20 dB. In Reed-Solomon and Block Coding cases one 1000 bits input

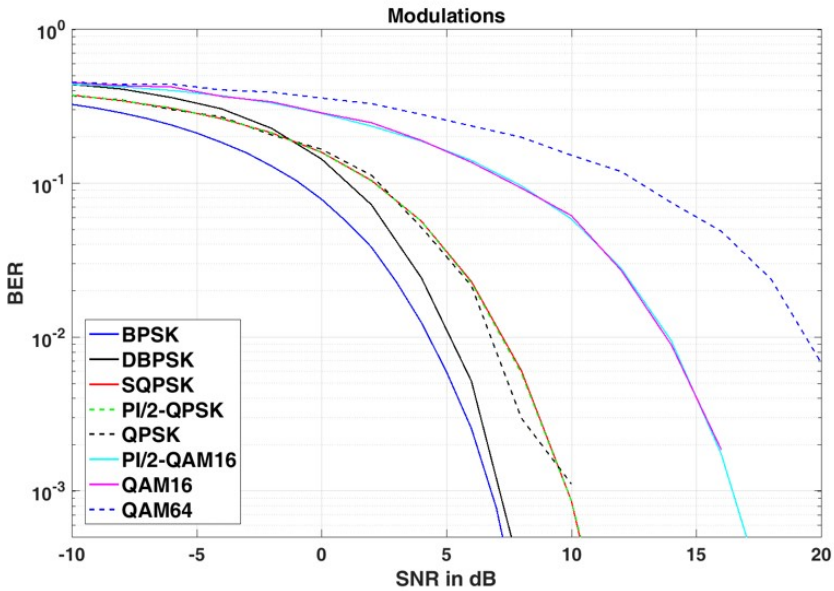


FIGURE 4.1: Modulation schemes BER curves.

word is used in 100 realizations in a SNR range of -10 to 20 dB. The results can be observed in the Figure 4.2.

### 4.1.3 Scrambler

The scrambler procedure is involved in the coding procedure independently if the signal is noisy or not. The function of the scrambler is to change the order of the symbols, consequently, it does not affect to the information itself.

The behavior of the scrambler at the receiver is able to reorder the sequence as it was generated in the transmitter correctly.

### 4.1.4 Interleaver

The interliever procedure is involved in the coding procedure independently if the signal is noisy or not. The function of the interliever is to change the order of the symbols, consequently it does not affect to the information itself.

The behavior of the interliever at the receiver is able to reorder the sequence as it was generated in the transmitter correctly.

### 4.1.5 Channel estimation

The channel estimation procedure is needed to accomplished the equalization. The preamble of every physical layer is standardized, therefore, it is information which the receiver knows in advance.

The preamble which compound the four PHY used in 802.11ad is formed by $G_a128$ and $G_b128$ signal. The Golay sequences autocorrelation properties are ideal

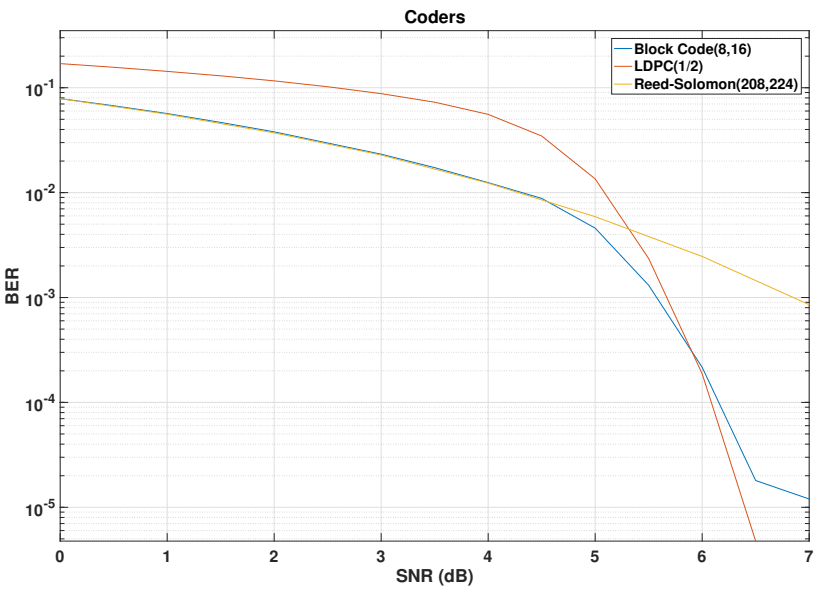


FIGURE 4.2: Reed Solomon and BC BER curves.

for signal detection applications. Furthermore, due to its similarity to AWGN regarding autocorrelation properties, the channel estimation could be accomplished using these properties.

$$R_x(k) = \sum_{j=0}^{N-k-1} x(j)x(j+k) \tag{4.1}$$

The sum of the autocorrelation function of a $G_a128$ and $G_b128$ results in Dirac delta. If the preamble is transmitted the received signal is:

$$R_{G_a128}(k) + R_{G_b128}(k) = 2L\delta(k) \tag{4.2}$$

$$r_a = G_a128 * h,\ r_b = G_b128 * h \tag{4.3}$$

If the received signal is correlated with the preamble standardized, the results is:

$$R_a = r_a * G_a = G_a * h * G_a = R_{G_a} * h \tag{4.4}$$

$$R_b = r_b * G_b = G_b * h * G_b = R_{G_b} * h \tag{4.5}$$

Therefore, the channel impulse response can be estimated comparing the autocorrelation properties of the transmitted preamble with the correlation between the preamble and the received signal to estimate the channel.

$$R_a + R_b = R_{G_a} * h + R_{G_b} * h = (R_{G_a} + R_{G_b}) * h = 2N\delta * h = 2Lh \tag{4.6}$$

After 15000 repetitions in a range of 1 to 30 SNR values the results are shown in the Figure 4.3.

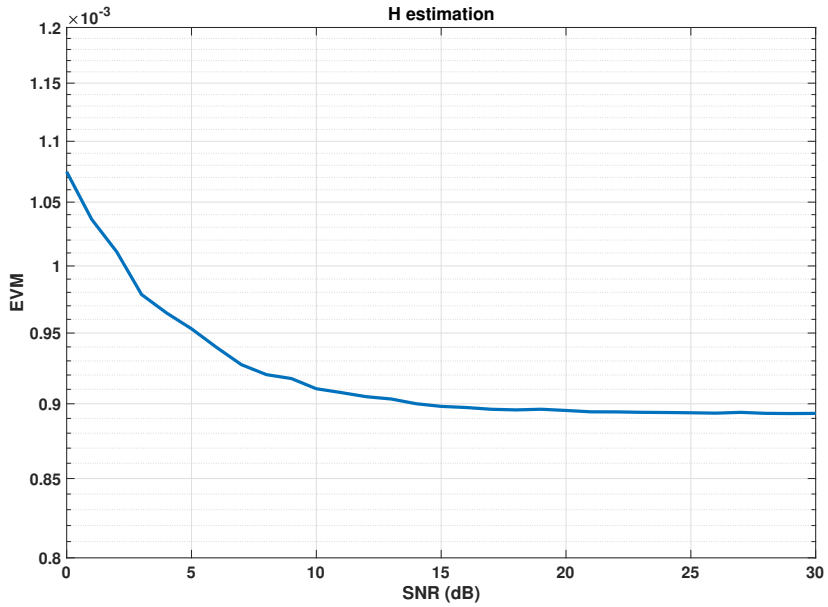


FIGURE 4.3: Channel estimation performance.

### 4.1.6 Equalization

The equalization procedure is intended to correct the signal distorted added by the channel. Equalizers are used to render the frequency response [7]. The actual waveform of the transmitted signal must be preserved, not just its frequency content. Equalizing filters must cancel out any group delay and phase delay between different frequency components.

The procedure used to correct the signal interference is explain as follows. Two different equalization procedures are used depending of the physical layer used for data transmission application. It must be considered that this procedure is only used in data transmission application where only the preamble of the signal received is standardized.

The equalization procedure is treated differently depending on the PHY which is detected. The OFDM symbols are appended with a cyclic prefix, this cyclic prefix permits equalize every packet independently equalizing each spectrum component per packet. Nevertheless, the rest of the PHY do not posses that property, therefore, the signal is convolved with the inverse response of the channel estimated. The mathematical procedures used in each physical layer are presented.

OFDM: As it is explained the equalization procedure is accomplished per packet, the number of packets can be deducted due to the length of the signal. It must be multiple of the down sampling factor multiplied by 640 due to it is the standardized number of carriers.

Firstly, the signal is divided in packets and the FFT is applied to each of the packets. After the FFT is divided by FFT of the channel to obtain the frequency expression of the equalize signal. Finally, the IFFT is used per packet and concatenated.

CL, SC, LPSC: The first requirement is to calculate the inverse response of the channel. Calculating inverse matrix is highly computational cost, therefore, the inverse can be done segmenting the matrix in several parts and make the inverse response of each of them independently of each other.

After calculating the inverse matrix, the signal received is multiplied with the inverse matrix. It must be considered that the multiplication is possible if the channel matrix is considered as a Toeplitz matrix.

In the Figure 4.4 the performance of the equalizer for OFDM is shown. As it can be observed, the MSE (Mean Squared Error) is higher in low SNR as it is expected due to the noise level. In low SNR conditions as it is observed in the channel estimation the quadratic error could be considered low, therefore, the error is introduced by the equalizer.

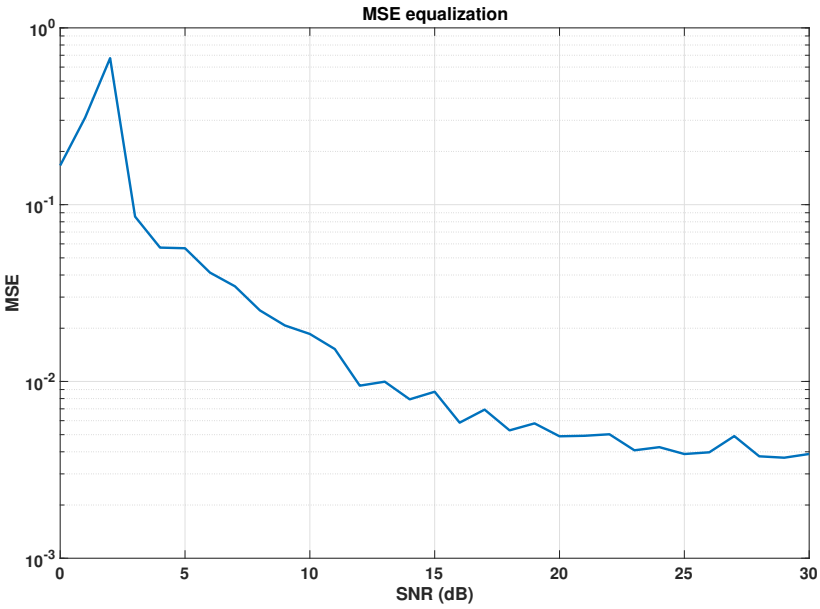


FIGURE 4.4: OFDM equalizer performance.

## 4.2 System tests

### 4.2.1 Detection

Signal detection theory is a means to quantify the ability to discern between information-bearing patterns and random patterns that distract from the information.

According to the theory, there are a number of determiners of how a detecting system will detect a signal, and where its threshold levels will be. The theory can explain how changing the threshold will affect the ability to discern, often exposing how adapted the system is to the task, purpose or goal at which it is aimed.

It is assumed two hypothesis in the case of making a decision between two hypotheses, H0 absent, and H1 present, in the event of a particular observation, a classical approach is to choose H0 when p(H0 | y) > p(H1 | y) and H1 in the reverse case. In the event that the two a posteriori probabilities are equal, one might choose to default to a single choice (either always choose H0 or always choose H1), or might randomly select either H0 or H1. The a priori probabilities of H0 and H1 can guide this choice. The stochastic of the hypothesis considered are:

$$H_0\ (0, \sigma^2) \tag{4.7}$$

$$H_1\ (\epsilon, \sigma^2) \tag{4.8}$$

The Bayes theorem concludes in the following two equations which quantify the ration between the probability of both hypothesis.

$$\frac{p(y|H_1)}{p(y|H_0)} = L(x) \tag{4.9}$$

The two hypothesis mentioned are the absent and the present of a signal. Both signals are summed by an AWGN signal as the stochastic indicates. Therefore, the false alarm and the miss probability are not null and a theory to establish the threshold to decide which is hypothesis is chosen must be used.

Following a Neyman-Pearson strategy, the (LLR) log likehood ratio L(x) is a continuous random variable and hence randomization is an issue. Moreover, comparing likehood ratio L(x) to a threshold $\gamma$ remains to choose a threshold to achieve a ($P_{fa}$) false alarm probability $\alpha$. Using the conditional distribution of H0 we obtain the expression of the Formula 4.10.

To achieve a specific false alarm probability the threshold to be chosen as it is expressed in the Formula 4.11.

$$P_{fa} = P\{x > \gamma^{'}|H_0\} = Q(\frac{\gamma^{'} - \mu_0}{\sigma}) \tag{4.10}$$

$$\gamma = \mu_0 + \sigma Q^{-1}(P_{fa}) \tag{4.11}$$

The $\sigma$ values is calculated from the SNR with the next expression.

$$\mu_0 = 10^{-\frac{SNR}{10}} \tag{4.12}$$

The $\mu_0$ are values calculated base on the correlation between the transmitted and received signals. The $\mu_0$ value is the maximum peak of the correlation function.

The average of the autocorrelation function achieved with the reference signal transmitted and the signal received is compared with the threshold.

The signal detection simulation objective is obtain the Signal Detection Probability curves in order to find out how the receiver detects the upcoming signal in different SNR environments.

The procedure to test the signal detection of the system is based on simulated signal + noise and noise packet generation. In the case of signal + noise the physical layer is defined and in the noise signal a simulated physical layer is related is used.

Consequently, the present or the absent of signal is known.

The signal + noise and noise packets are generated with different levels of SNR and the autocorrelation function between the packets and the expected signal is accomplished. If the autocorrelation of the signal + noise packet is evaluated and the detector decides that there is no signal it is a cause for error detection. It is also a cause for an error detection (false alarm) if the autocorrelation of the noise packet is evaluated and the detector decides that there is a signal present.

The length of the signals is different depending of the MCS, this aspects is critical related with the autocorrelation properties of the signal. Hence, a longer signal such as CL (MCS0) signal has a better performance than a SC signal. In order to achieve the average performance of the system independently of the MCS, the simulations are considering all the MCSs to calculate the Signal Detection Probability.

The simulation settings cover all the 32 MCS available fixing a wide range of false alarm probabilities for each SNR in a range of -5 to 10 dB with a false alarm order probability in a range of -12 to -1. The procedure to calculate the Signal Detection Probability curves is based on assess the quantity of correct detections in every SNR and False Alarm probability values over all realizations. A correct detection consists of a positive detection if a signal is received as well as a no positive detection if a signal is not received (noise).

- Number of MCS = 32
- SNR = -5 to 10 dB
- False alarm probability = [$10^{-12}$,$10^{-11}$, ... ,$10^{-i}$ , ... ,$10^{-2}$,$10^{-1}$].
- Repetitions = 100

After evaluation 32 MCS, the Figure 4.5 shows the Signal Detection Probability curve for detection using the preamble and the Figure 4.6 shows the Signal Detection Probability curve for detection using the entire signal.

### 4.2.2 Ideal data transmission

The individual simulations show that every individual functionality performs correctly. Each MCS packet is treated using different modes of the individual functionalities, then the transmission and reception chain integrates every individual functionality as it is explained in section 4.1.1 with the correspondent input parameters.

The transmission packets are generated and stored alongside the maximum of the signal and the bare data before coding procedure to tackle the quantization procedure explained in section E.2.

The receiver is able to load the stored packets and add an AWGN signal with different SNR and the reception procedure is done.

Testing the performance of the reception is firstly approach introducing no noise signal to find out that no mistakes are committed in the procedures, and once the

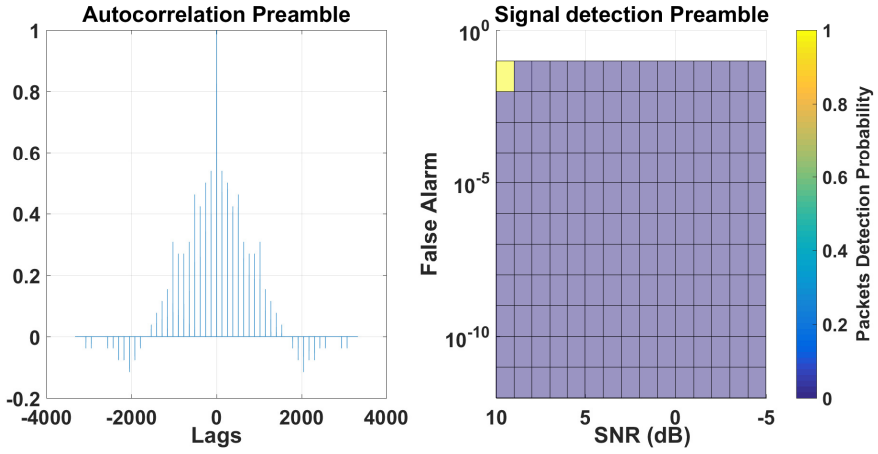


FIGURE 4.5: Preamble autocorrelation and Signal Detection Probability Preamble detection.

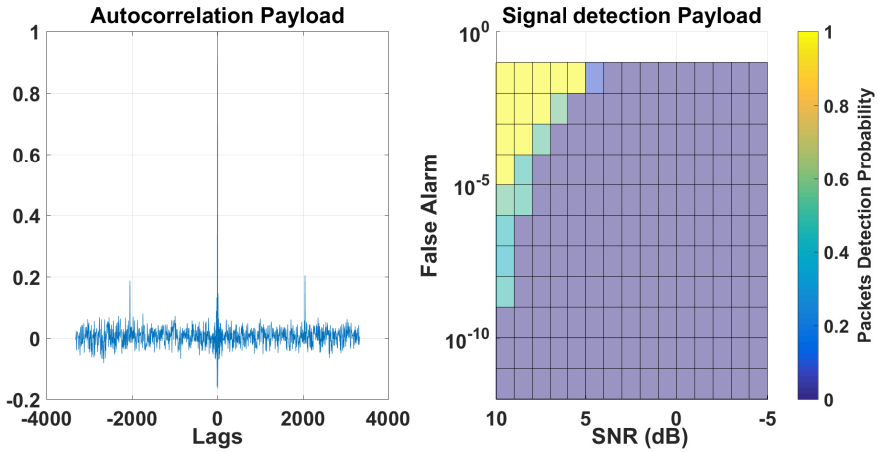


FIGURE 4.6: Payload autocorrelation and Signal Detection Probability Payload detection.

performance is checked the noise signal is introduced.

Every MCS is tested without adding noise in the packet in 100 realization, the results expected in every test shows that the error signal which compares the data decoded and the original data is null.

### 4.2.3 AWGN channel transmission

Every MCS is tested adding AWGN signal to the transmitted packet to imitate a real transmission with no fading. The objective of the simulation is to obtain the BER vs SNR curves of the MCS.

The transmitter is able to generate every packet in an affordable simulation time. However, due to the lack of optimization of the receiver, the decoding procedure for the signals employs an unfordable simulation time to decode more than 1023 octets long sequences if accurate results are required, consequently, every packets generated is fixed to 1023 octets due to it is affordable time simulation and its length

enough to acquire reliable results.

A packet of 1023 octets of bare data and the redundancy added by coders has an order of $10^4$ at most. Consequently, obtaining error rates of $10^4$ with a single realization is not reliable. To solve this situation, 30 sets of each MCS signals. Hence, 960 with different data are generated.

Additionally, 100 noise realizations per signal are done. As a results, 96000 realizations would be done. Nevertheless, the simulation time was calculated based on 1 realization simulations and the results would be obtained after 32 days of simulation, consequently, the higher throughput mode of each physical layer are measured, MCS 0, 12, 24, 31 reducing the simulation time to 4 days. The results of the simulations are observed in the Figure 4.7.

As it can be observed in the Figure 4.7 the BER curve correspond to different MCS which the Single Carrier MCS 12, Low Power Single Carrier MCS 31, and OFDM MCS 24, the throughput of the OFDM signal is higher than the other Single Carrier modes. The throughput of the OFDM MCS 24 is the higher standardized which is 6756.75 Mbit/s and the modulation order is 6, consequently, the BER is higher for higher SNRs as it can be observed.

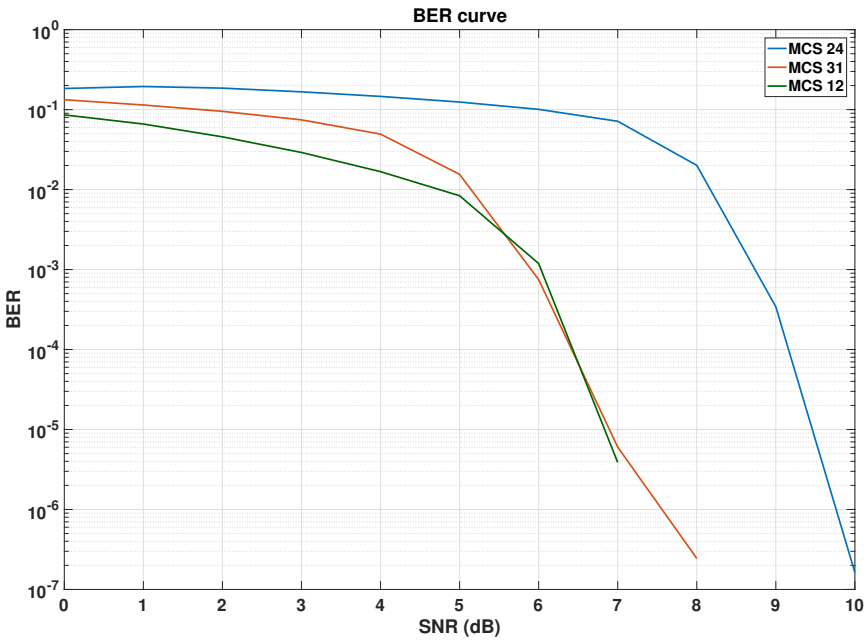


FIGURE 4.7: SC, LPSC, and OFDM physical layer performance

In the Figure 4.8 the percentage of missed packets is shown per MCS. It can be conclude that the performance is similar in all of them due to the number of missed packets depends on the header codification which is similar in SC, LPSC, and OFDM PHYs.

The simulation of the performance of this MCS 0 is more difficult to accomplished correctly. The signal is modulated with a 1 order differential modulation

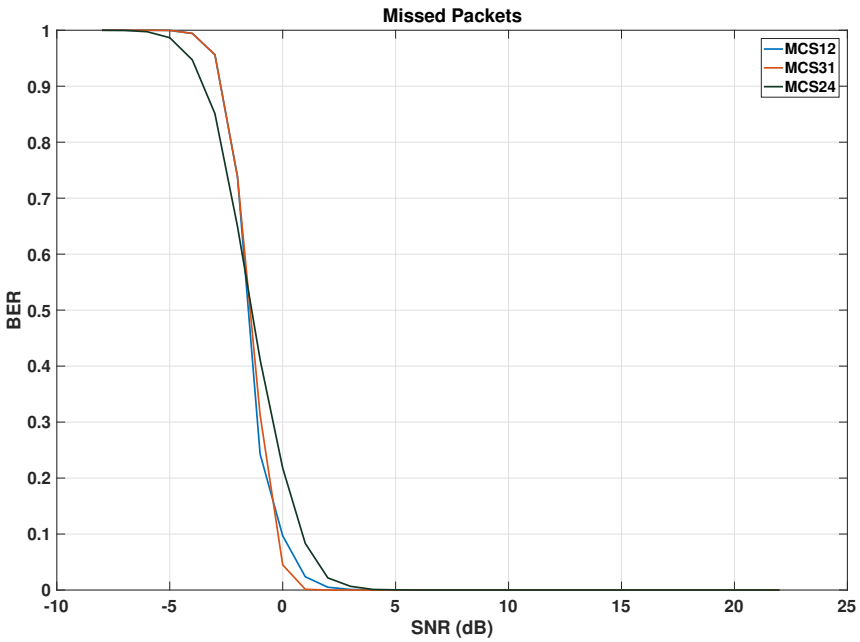


FIGURE 4.8: Missed packets in SC,LPSC,and OFDM physical layers

(3 dB over non.differential modulation) and the stronger coding rate available ($\frac{1}{2}$ - LDPC), and spread with a factor of 32 and the coding gain is 15 dB as it is shown in the section 2.2.4. Therefore, a higher number of simulation is required in lower SNRs level than in the other physical layers, then, the real performance of the MCS 0 is difficult to observed due to the simulation time required.

The MCS 0 is evaluated in 100 realizations per SNR and 30 packs of signals. The range of SNR evaluated are -25 to 5 dB. The approximation to the performance of the MCS 0 can be observed in the Figure 4.9.

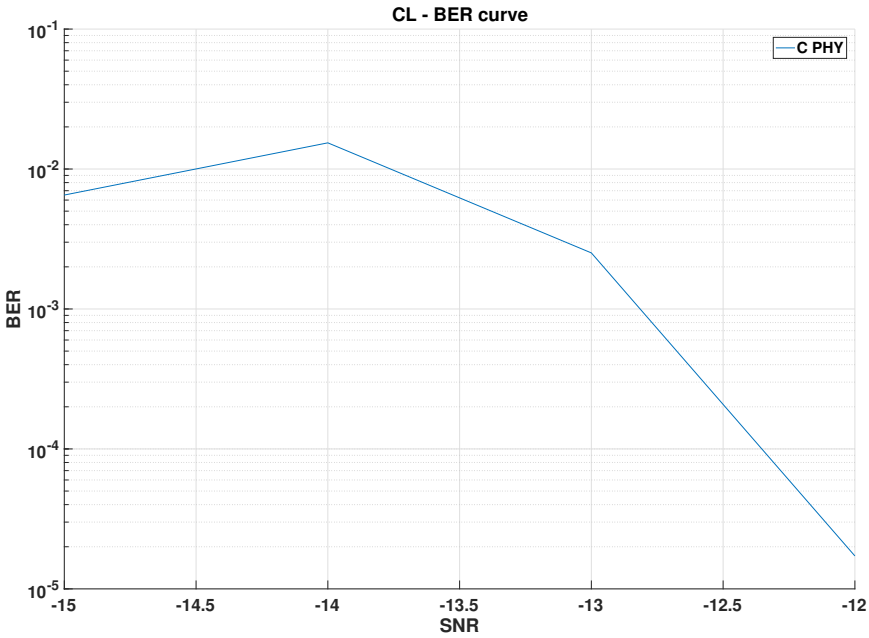


FIGURE 4.9: CL physical layer performance

# Chapter 5

# Measurements

The simulations conclude that the performance of the system is as it is expected. Therefore, the packets generated by the transmitter are sent through a real environment with low fading, due to it was simulated supposing an AWGN environment. The I/Q signals are recorded by a spectral analyzer to be treated and compared with the performance of the system simulated and in a real environment.

In this section the setup used in the system is presented alongside the parameters set to assure the well performance of the system, and the results obtained for radar and data transmission experiments.

## 5.1 Setup

The apparatus used for this project consist of an arbitrary waveform generator, a signal generator to generate the carrier, an attenuator to control the signal amplitude, a 60 GHz up-converter, an oscilloscope, and a spectrum analyzer to record the received signals. The Figure 5.1 shows the setup.

The devices which form the setup are listed:

- Keysight M8195A Arbitrary Waveform Generator [10].
- R&S®SMA100A Signal Generator [11].
- R&S®RTO2000 Digital Oscilloscopes [12].
- R&S®FSW-K95 Signal and Spectrum Analyzer [13].
- Pasternack. 60 GHz Transmitter (Tx) Waveguide Module [14].

## 5.2 Setting parameters

The initial sets to tackle the measurements are explained as follows:

### 5.2.1 Recording length

The length of the signal is adjusted to the length of the signal generated in every MCS. Apart of the signal, it is necessary analyzing the noise level introduced in every realization. Therefore, it is recorded 2560 more null samples than the length of the signal in order to assure the proper recoding of the signal and to analyze the noise added by the channel.

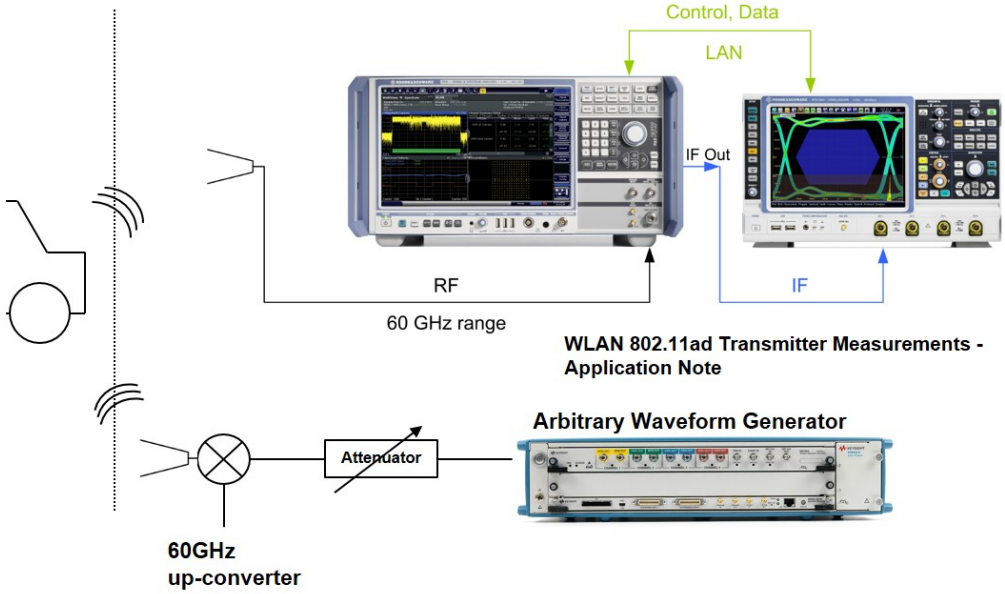


FIGURE 5.1: Setup scheme

### 5.2.2 Output frequency

The central frequency selected is the central frequency of the channel 3 specified in the 802.11ad standard and available in Europe, the center frequency is then 62.64 GHz. The frequency is synthesized through a digital programmable divider using a reference frequency of 308.571 MHz. The limitations in accuracy in the synthesizer does not permit generate a carrier signal exactly at 62.64 GHz, therefore, 62.639913 GHz signal is generated.

### 5.2.3 Sample frequency

The sample frequency established by the standard is 2.64 GHz for OFDM. Nevertheless, the waveform generator is programmed to work in a range of 13.44 to 16.25 GHz when 4 channels are sampled. Therefore, the up-sampling procedure whit a factor of $N_{up}$ = 6 is used as it is explained in the Appendix E.3 reaching a sample frequency of 15.84 GHz

The recoding sample frequency at the receiver is multiple of the sampled frequency established in the standard. However, this sampled frequency cannot be exceed to 10 GHz, therefore, up sampling and down sampling factor cannot be equal. The down sampling factor chosen is $N_{down} = 3$, then, 7.92 GHz is the sampled frequency to record the data received.

### 5.2.4 Input power level

The amplitude of the signal is controlled through an attenuation factor, but the input power generated by the waveform generator is constant. The input voltage set is 1V, but it is 10 dB attenuated at the output of the waveform generator in order to not exceed the maximum ratings of the transmitter of -16 dBm.

### 5.2.5 Signal Packets

The packets are generated in 30 sets with different random data, the intention of this sets is evaluate the effects of the channel independently of the payload waveform characteristics. These sets and 100 realizations per packet offer us 3000 measurements per attenuation level.

### 5.2.6 Attenuation values

The attenuation values are set to attenuate the signal in order to evaluate the signal with lower signal amplitudes. The attenuation is set following two criteria. The first criteria is avoiding the overload of the IF filter of the spectrum analyzer, this criteria with the input power conditions establish the attenuation at most at 6 dB for I and Q channels. The second criteria is the non-linear region of the power amplifiers which form the transmitter. Following the transmitted specifications it is deducted that the linear region could be reached with 16 to 20 dB attenuation, therefore, to analyze the influence of the noise and the non-linear effects in the packets the attenuation values set are in the range of 6 to 40 dB attenuation.

### 5.2.7 Trigger level

The trigger signal is an square pulse of 150000 samples up and 150000 samples down. The sample frequency is 2.64 GHz, but the signal is up sampled by a factor of 6, therefore, the duration of the trigger is 9.45 $\mu$s and the trigger level is set to 100 mV. These parameters are fixed for every physical layer.

## 5.3 Experiments

In this section the two different experiments which were accomplished and the issues faced are described. The first point describes the procedure to measure the signals, the second point describes the measurements with all the cars equipped and the vehicle is able to received a signal and the payload received is not know by the receiver (Data transmission measurements), and the third point describes the one car equipped case where the signal reflected in a car which is not 802.11ad equipped is received by the car which is transmitting. As a consequence, the receiver knows the payload (Radar measurements).

### 5.3.1 Signal measurement procedure

The procedure to measure the different 32 packets and each set is described as follows:

1. The transmitter generates the 32 different packed correspond to the 32 MCS standardized. For every kind of packet 30 sets of packets are generated resulting in 960 packets. It must be observed that the packets are stored in an 8 bits binary file which does not store complex values, therefore, the real values are stored in one file and imaginary values in other file. As a result, 1920 packets with their respective triggering.

2. The up-converter is set to the central frequency specified and each couple of imaginary and real values packets are loading independently alongside their triggering signals.

3. The attenuation and number of repetition values are set to accomplished several noise realization in every SNR. Therefore, more data is stored and the results obtained would be more reliable.

4. The spectral analyzer reads the realizations of every packet and the waveform recorded is stored in order to be decoded.

### 5.3.2 Data transmission measurements

The data transmission application is exclusive for the two equipped vehicles. The data transmitted is received distorted by the channel and the non-linear distortions introduced by the power amplifiers.

As it is explained in the point 3 in the measurement procedure the signal is attenuated in order to modify the (Signal-to-interference-plus-noise ratio) SINR conditions due to the noise level is always constant. The formula to calculate the SINR is shown.

$$\text{SINR} = 10\log_{10}\left(\frac{P_{signal}}{P_{noise}}\right) \tag{5.1}$$

Where $P_{signal}$ is the average power of the signal recorded before equalization and $P_{noise}$ is the average power of the noise. The procedure to measure the noise average power is based on recording extra samples between packets.

The simulations are done based on an SNR level (Interferences not simulated) and the measurements are based on an attenuation level. Therefore, an equivalence between attenuation and SINR must be found. The SINR calculated using the Formula 5.1 per attenuation value is plotted against attenuation. This equivalence is shown in the Figure 5.2. As it can be observed, the lower attenuation values are related with the higher SINR values due to the average signal power is high; furthermore, the higher attenuation values are related with lower SINR values due to the average signal power is low.

The packets which are measured in a first approach are the MCS 24 packets, whose behavior in low SNR is poorer than the other OFDM modes due to the high modulation order.

After obtaining the data related with the SNR measured in every PHY, it can be concluded that the modulation orders of 6 and 4 bits can be discarder due to both modulation order requires more than 8 bits to perform correctly. Therefore, the 4-QAM modulations are measured. In the Figure 5.3 the 4-QAM constellation obtained is compared with the ideal one.

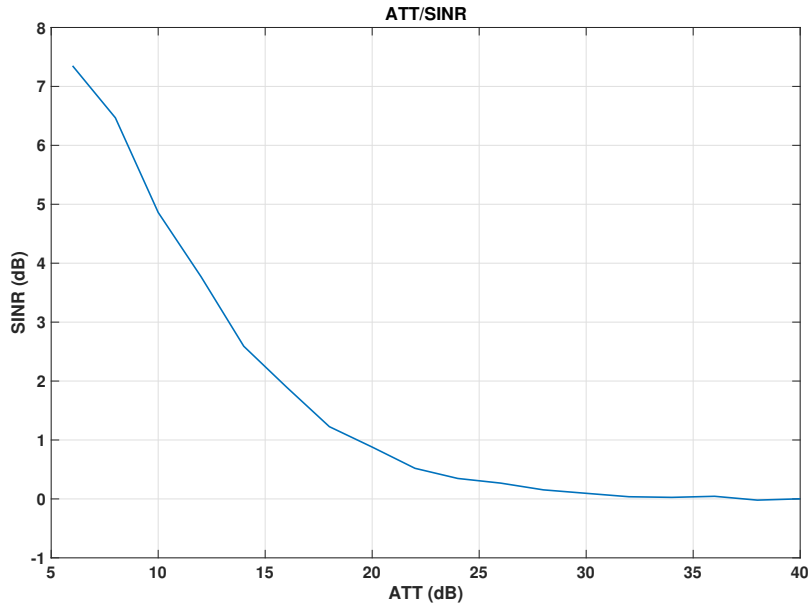


FIGURE 5.2: Relationship SNR/ATT.

### 5.3.3 Radar measurements

The radar application is used in the on car equipped case, the objective is to determine the distance between vehicles base on the propagation time required to transmitted signal until it is received in the car which transmits.

We can infer during measurements that we are only receiving 802.11ad packets, since the radar application can be tested without the detection signal application influence.

The signal received is convolved whit the channel and additive noise. As a consequence, the signal have to be equalized to recover the signal. The first packet is compared with the signal transmitted, therefore, a correction factor per sample can be used. The correction factor per channel is used in every packet, it is supposed that the channel is constant during the transmission of all the packets. Consequently, the only effects which are no corrected in equalization in the remaining packets are the non-lineal setup effects and the additive noise. However, this equalization process is repeated once per attenuation. This equalization technique is call data-aided estimation.

The results after measurements shown that the data is correctly decoded and the BER curves fits with the simulations as it is shown in the Figure 5.5 for OFDM and in the Figure 5.4 for SC. However, the number of packets missed shown a different distribution as it is done in simulations. The missed packets distribution shown that for low SNR levels there is a peak in the number of packets in comparison with the higher SNR levels.

The tendency for high SNR to reduced the missed packets percentage could be explained by the reduction of the noise level in comparison with the amplitude of

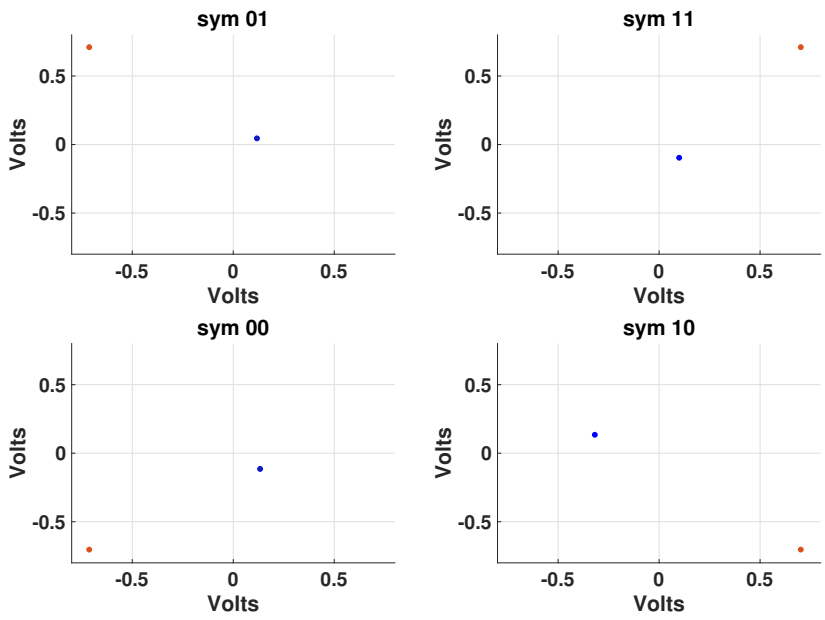


FIGURE 5.3: 4-QAM Constellation.

the signal. However, the peak in the high SNR values could be explained with the $3^{rd}$ order intermodulation interferences, the reason for this phenomenon is that high SNR are related with low attenuation values, as a consequence, the signals saturate the power amplifiers producing these intermodulation products. Therefore, these curves can show a of the behavior of the noise and the intermodulation interferences. The peaks generated by interferences are more numerous in OFDM due to is more likely getting interferences in OFDM than in SC. The representation for OFDM of this phenomena is the Figure 5.5 and for SC the Figure 5.4.

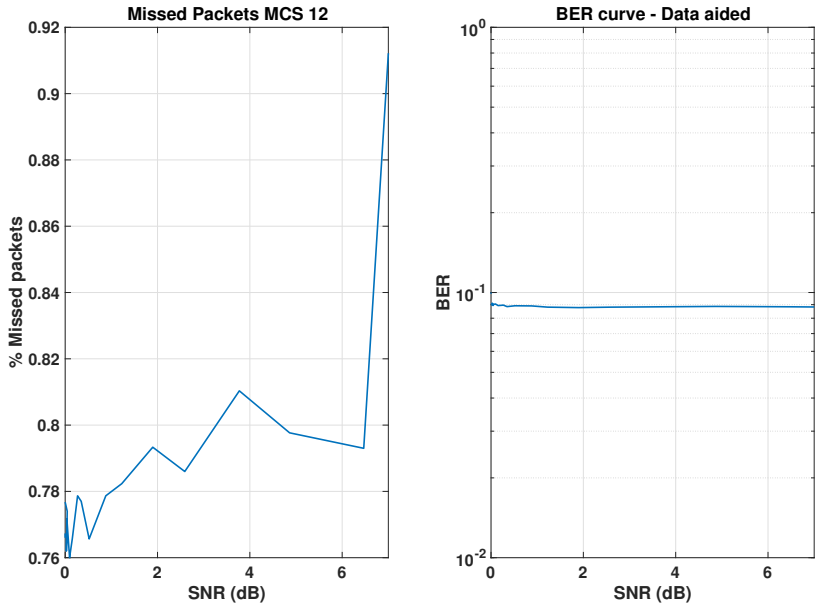


FIGURE 5.4: BER curves and Missed Packets for SC - Radar application.

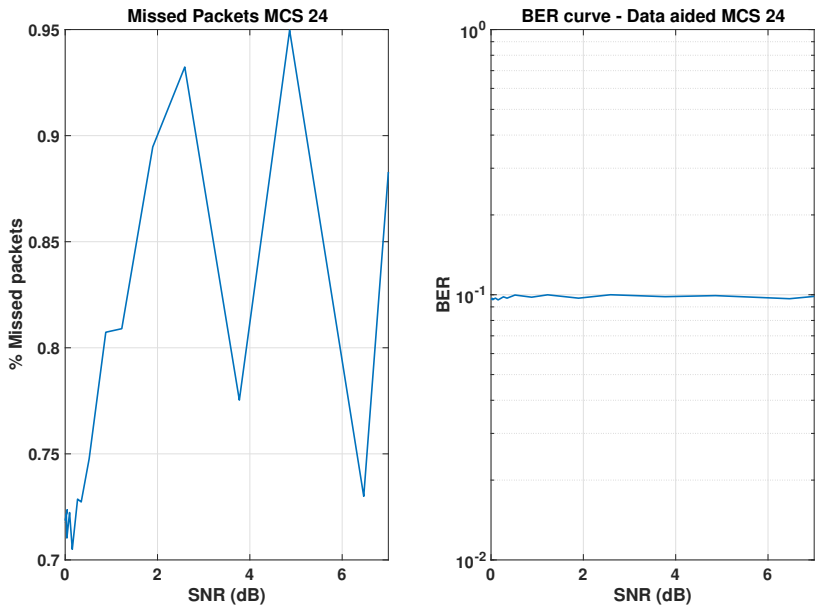


FIGURE 5.5: BER curves and Missed Packets for OFDM - Radar application.

# Chapter 6

# Conclusion

The 802.11ad project is concluded simulating and sending standardized packets through a real setup in order to prove the behavior of the system. The simulations were done taking in account the system partially and completed to prove the assumptions suggested along the thesis. It can be concluded that the performance of the transmitter is adequate due to the comparison with the theoretical values which should be reached in every modules such as coders and modulators.

After checking that the individual performance of every modules works properly it can be conclude the well performance of the system in a controlled flat channel. The weaker coded MCS of every physical layer are tested to check with the minimum execution time possible. The error rate per MCS evaluated is tested in order to compare the capacity of the physical layer due to their throughput is different.

After concluding that the simulations show a proper performance of the system, some other conclusion could be deducted from other applications.

It can be deducted that the payload performs better in detection applications than the preamble only. As it can be observed in the Figure 4.6 the error probability that can be reached in 7 dB SNR could be considered despicable for a good detection probability, therefore, considering the payload assumption, the system is viable to detect the position of other vehicles.

High order modulation MCSs compact the sequences in symbols with a wide range of values, therefore, the output sequences are shorter. This aspect can be meaningful for radar applications, because as it was seen it is necessary having a long signal to have better autocorrelation properties and ,then, better detection characteristics. As a consequence, it should be given higher priority for both applications to lower MCS modes in order to increase the security in vehicular environments, despite the lower throughputs.

The last aspect that should be considered is that the system is very sensitive in the typical SNR conditions to intermodulation products. As it is shown in the Figures 5.4 and 5.5 the 20% of the SNR values in Single Carrier modes and 70% of the SNR values for OFDM are dominated by interferences over noise. The most meaningful factor to variate the SNR is the distance between cars. Therefore, the performance of the system could decay if the distance between cars is decrease in a short period of time if OFDM MCSs are used. This aspect could be critical for safety conditions of the system.

# Chapter 7

# Bibliography


1. Sarah J. Johnson, (2001). Introducing Low-Density Parity-Check Codes School of Electrical Engineering and Computer Science, The University of Newcastle, Australia.

2. Ki Seol Kim, Kwangmin Hyun, Chang Wahn Yu, Youn Ok Park, Dongweon Yoon, and Sang Kyu Park, (2006). General Log-Likelihood Ratio Expression and Its Implementation Algorithm for Gray-Coded QAM Signals.

3. IEEE Computer Society, (2012). Part 11: Wireless LAN Medium Access Control (MAC) and Physical Layer (PHY) Specifications. Amendment 3: Enhancements for Very High Throughput in the 60 GHz Band.

4. Rohde & Schwarz, (2012). 802.11ad - WLAN at 60 GHz A Technology Introduction.White Paper.

5. Valentin Savin, CEA-LETI, MINATEC, (2008). Min-Max decoding for non binary LDPC codes.

6. Stephen Wicker, (1995). Error Control Systems for Digital Communication and Storage.

7. Markus Rupp and Jose.A Garcia Naya, (2012). Equalizers in mobile communications: Tutorial 38 Part 38 in a series of tutorials on instrumentation and measurements.

8. Vutha Va, Takayuki Shimizu, Gaurav Bansal and Robert W. Heath Jr. (2016). Millimeter Wave Vehicular Communications: A Survey.

9. Alan V. Oppenheim, Ronald W.Schafer, Jhon R.Buck (1999). Discrete-Time Signal Processing.

10. Keysight Technologies, (2016). Keysight M8195A Arbitrary Waveform Generator Revision 2.

11. Rohde & Schwarz, (2016). R&S®SMA100A Signal Generator User Manual.

12. Rohde & Schwarz, (2017). R&S®RTO Digital Oscilloscope User Manual.

13. Rohde & Schwarz, (2008). R&S®FSW-K95 802.11ad Measurements User Manual.

14. Pasternak, (2013). 60 GHz Transmitter Waveguide Module.

# Appendix A

# Scramble, demodulation, and Checksum

## A.1 Scrambling

### A.1.1 Scramble part

The header and data fields following the scrambler initialization field (including data padding bits) shall be scrambled by XORing each bit with a length 127 periodic sequence generated by the polynomial.

$$S(x) = x^7 + +x^4 + 1 \tag{A.1}$$

The former polynomial is represented as a LFSR with 7 slots.

The header bits, with the exception of the first 7 bits for SC and OFDM and the 5 five bits for control PHY, are placed one after the other, bit 7 first (bit 5 first for CL PHY). The octets and the pad bits shall be placed into a bit stream with bit 0 (LSB) of each octet first and bit 7 of each octet (MSB) last.

### A.1.2 Descramble part

The receiver must descramble the header and the payload. As it is implemented using a XOR operator, the only requirements are the same scramble state and the same input word length used in the transmitter sequence in order to generate at the output the right remain scrambling state to be used in further scrambling procedures.

## A.2 Demodulation

Max-Log MAP is the algorithm used to implement soft decision method throw LLR in demodulation procedures [2]. LLR establishes the probability of each symbol received to be in a specific group of k bits, where k is the logarithm in base 2 of the modulation cardinality.

A LLR value is required per bit, since two possible values are considered in the ratio, 1 and 0. Like-hood ratio is shown:

$$L = ln(p(b_i = 1|r)) - ln(p(b_i = 0|r)) \tag{A.2}$$

Bayes theorem is used based on that the subset of bits is known. An AWGN function distribution can be expressed.

$$p(r|s = s\ ) = \frac{1}{\pi\sigma_n^2} e^{\frac{-((r-s)^2}{\sigma_n^2})} \tag{A.3}$$

$$LLR = ln(\sum e^{\frac{-(r-s)^2}{\sigma^2}}) - ln(\sum e^{\frac{-(r-s)^2}{\sigma^2}}) \tag{A.4}$$

Considering that the sum of exponents is dominated by the largest component:

$$Ln(sum(e^{x_1})) = max(x_1) \tag{A.5}$$

$$LLR = -\frac{1}{\sigma_n^2}(min(|r-s|^2) - min(|r-s|^2)) \tag{A.6}$$

## A.3 Checksum

Checksum procedure involves a small-sized datum derived from a block of digital data for the purpose of detecting errors which may have been introduced during its transmission or storage. As it is set in the header the checksum sequence is set in the header in the HCS field. To generate this sequence a CRC 16 CCITT is used, the scheme of this CRC is based on a polynomial model implemented in a shift register. The register is initialized at 0XFFFF and data is shifted and xored with the shift register states 1, 5, 12, and 16 and extracted. The block diagram of the CRC process is shown in the Figure A.1.

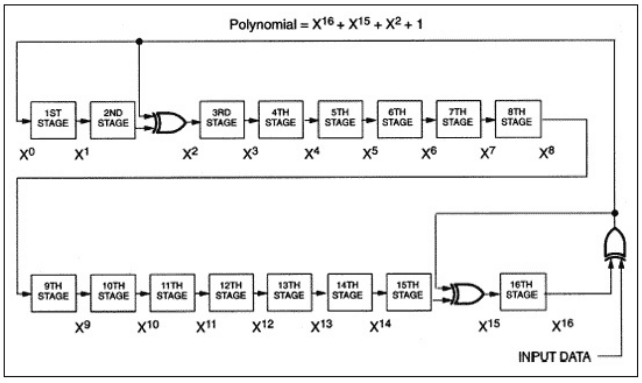


FIGURE A.1: CRC Block diagram.

# Appendix B

# Evaluation of the transmitter. Metrics

The performance of the system is tested using metrics which compare the measured values with the ideal ones. In this case EVM accuracy test is performed in order to check that the signals are generated properly. Omitting phase, DC offsets, and other phenomenon due to assuming perfect synchronization, RMS averages is done to measure the EVM. The EVM is considered in several SNR values, but it must be considered that the SNR in the transmitter could be considered high.

EVM requirements per each MCS is specified in the standard. The formulas applied per PHY are shown. It is must be noticed that the LPSC has not EVM requirements specified.

## B.1 CL

The RMS average formulas consider the Euclidean distance between the constellation received and the ideal constellation. The symbols considered are extracted from the spread form. MCS 0 is modulated with $\frac{\pi}{2}$ - DBPSK constellation. Hence, 1 bits constellation is used. The RMS is averaged by the average power of the constellation calculated as it is shown in B.4.

## B.2 SC

The RMS average formulas consider the Euclidean distance between the constellation received and the ideal constellation. The symbols considered are extracted from the non- guard sequence part of the symbols stream. MCS 1 – 5 $\frac{\pi}{2}$ - BPSK constellation is considered. Hence, 1 bits constellation is used, MCS 6 – 9 $\frac{\pi}{2}$ - QPSK constellation is considered. Hence, 2 bits constellation is used, and MCS 10 – $\frac{\pi}{2}$ - 16-QAM constellation is considered. Hence, 4 bits constellation is used. The RMS is averaged by the number of the carriers and the average power of the constellation calculated as it is shown in B.4.

## B.3 OFDM

The RMS average formulas consider the Euclidean distance between the constellation received and the ideal constellation. The symbols considered are extracted from

every carrier and compared with the ideal constellation. MCS 13 – 14 SQPK constellation is considered. Hence, 4 bits constellation is used, due to 2 streams of symbols to 2 group of carriers is implemented, MCS 18 – 21 16-QAM constellation is considered. Hence, 4 bits constellation is used, and MCS 22 – 24 64-QAM constellation is considered. Hence, 6 bits constellation is used.

## B.4 Average constellation power

Average power constellations consider the complex amplitude of all the symbols of the constellation. The standard average power constellations for the 1, 2, 4, and 6 order modulations which are considered is:

- P1 = 1 units.
- P2 = 1 units.
- P4 = 1.8 units.
- P6 = 2.33 units.

# Appendix C

# Golay sequences

As it was explained in the last section, the training sequences are mainly intended to estimate the channel, consequently, they must be standardized in order to be known either by the transmitter and the receiver. Furthermore, the sequences used to implement these fields must have good autocorrelation properties in order to improve the detection probability of the signal, the presence or not-presence of the signal. Golay sequences accomplished this properties since they are used to implement this fields and to assure the synchronization between the transmitter and the receiver. However, this aspect is further explained in the receiver section.

Autocorrelation properties of these sequences are improved with the length of the sequence, consequently, depending of the importance of the field for the detection, the length of the sequence is fixed, the bigger the importance the longer the sequence. The lengths of the Golay sequences used are 512, 128, 64, 32, and 8.

## C.1 Guard Insertion

Guard insertion is a sequence insertion between symbols in order to smooth the transition between them and to improve the synchronization between transmitter and receiver due to the sequences are known.

The sequences introduces are Golay sequences of different lengths depending on the physical layer.

### C.1.1 LPSC

Data is divided in block of 512 symbols and at the end of the number of symbols a Ga64 is introduced. Each 512 block is divided in 8 sub-blocks of 64 symbols, the first block is Ga64 sequence and the remaining blocks are divided in 56 symbols and G8 sequence in order to complete the 64 symbols.

### C.1.2 SC

Data is divided in 512 symbols blocks. Each 512 block is divided in a Ga64 sequence and 448 symbols in order to complete the 512 symbols.

# Appendix D

# Codification

In this section all coders which are used in the 4 different physical layers are explained. On the one hand, LDPC is used in Control Layer, Single Carrier, and OFDM. On the other hand, Block code and Reed Solomon is used in LPSC.

## D.1 LDPC coding/decoding

LDPC codes are block codes with parity-check matrices that contain only a very small number of non-zero entries [1]. It is the sparseness of H which guarantees both a decoding complexity which increases only linearly with the code length and a minimum distance which also increases linearly with the code length.

The biggest difference between LDPC codes and classical block codes is how they are decoded. Classical block codes are generally decoded with ML like decoding algorithms and so are usually short and designed algebraically to make this task less complex. LDPC codes however are decoded iteratively using a graphical representation of their parity-check matrix and so are designed with the properties of H as a focus.

### D.1.1 Encoding

Codewords must fulfill the following criteria. The former formula could conclude in a non-detection error in even error patterns. To deduce the influence in the error rate more redundancy is added depending on the structure of the parity matrix. Only n bits which form the codewords are data, n-k bits are parity bit to check possible mistakes. The parity matrix condition could be rewritten as it is shown: Consequently the following procedure is implemented:

$$H_1 \cdot s_{input} s_{paritybits} = H_2$$

TABLE D.1: Word sizes per coding rate

| Code Rate | Codeword size | Number of data bits |
|---|---|---|
| 1 | 672 | 336 |
| 2 | 672 | 420 |
| 3 | 672 | 504 |
| 4 | 672 | 546 |

$$s_{paritybits} = \frac{H_2}{H_1} s_{input}$$

### D.1.2 Decoding

The sum-product algorithm is a soft decision message-passing algorithm, the messages are representing probabilities. The sum-product algorithm is a soft decision algorithm which accepts the probability of each received bit as input. Considering likehood ratios in decoding procedure adds the advantage of a better performance than in hard decision as it was used in Reed Solomon decoding. In order to achieve a better performance SC, LPSC, and CL demodulator's outputs are likehood ratios instead of subset bits of 1s and 0s.

The sum-product algorithm iteratively computes an approximation of the MAP value for each code bit. The aim of sum-product decoding is to compute the maximum a posteriori probability (MAP) for each codeword bit $P_i = Pc_i = 1|N$ which is the probability that the i-th codeword bit is a 1 conditional on the event N that all parity-check constraints are satisfied. The extra information about bit I received from the parity-checks is called extrinsic information for bit i.

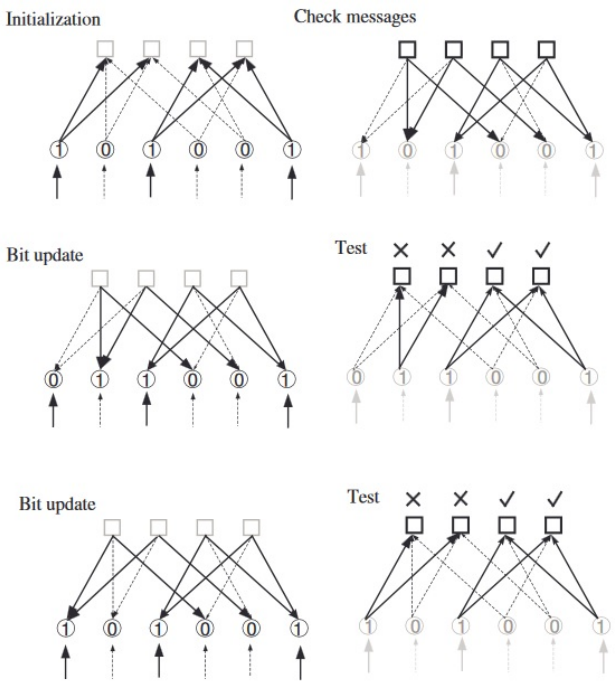


FIGURE D.1: LDPC correction procedure.

As it is shown in the Figure D.1, the algorithm computes several confirmations checking the data with the redundancy through a Tanner graph. The nodes check the priori probability to relate a data from a data node whit a check node, if the data is not correct the sign is flipped. After several iterations the data corrected is a posterior probability and the redundancy is discarded. The parity matrix used in the project are shown.

Rate 1/2 LDPC code matrix

$$\begin{pmatrix} 40 & -1 & 38 & -1 & 13 & -1 & 5 & -1 & 18 & -1 & -1 & -1 & -1 & -1 & -1 & -1 \\ 34 & -1 & 35 & -1 & 27 & -1 & -1 & 30 & 2 & 1 & -1 & -1 & -1 & -1 & -1 & -1 \\ -1 & 36 & -1 & 31 & -1 & 7 & -1 & 34 & -1 & 10 & 41 & -1 & -1 & -1 & -1 & -1 \\ -1 & 27 & -1 & 18 & -1 & 12 & 20 & -1 & -1 & -1 & 15 & 6 & -1 & -1 & -1 & -1 \\ 35 & -1 & 41 & -1 & 40 & -1 & 39 & -1 & 28 & -1 & -1 & 3 & 28 & -1 & -1 & -1 \\ 29 & -1 & 0 & -1 & -1 & 22 & -1 & 4 & -1 & 28 & -1 & 27 & -1 & 23 & -1 & -1 \\ -1 & 31 & -1 & 23 & -1 & 21 & -1 & 20 & -1 & -1 & 12 & -1 & -1 & 0 & 13 & -1 \\ -1 & 22 & -1 & 34 & 31 & -1 & 14 & -1 & 4 & -1 & -1 & -1 & 13 & -1 & 22 & 24 \end{pmatrix} \tag{D.1}$$

Rate 5/8 LDPC code matrix

$$\begin{pmatrix} 20 & 36 & 34 & 31 & 20 & 7 & 41 & 34 & -1 & 10 & 41 & -1 & -1 & -1 & -1 & -1 \\ 30 & 27 & -1 & 18 & -1 & 12 & 20 & 14 & 2 & 25 & 15 & 6 & -1 & -1 & -1 & -1 \\ 35 & -1 & 41 & -1 & 40 & -1 & 39 & -1 & 28 & -1 & -1 & 3 & 28 & -1 & -1 & -1 \\ 29 & -1 & 0 & -1 & -1 & 22 & -1 & 4 & -1 & 28 & -1 & 27 & 24 & 23 & -1 & -1 \\ -1 & 31 & -1 & 23 & -1 & 21 & -1 & 20 & -1 & 9 & 12 & -1 & -1 & 0 & 13 & -1 \\ -1 & 22 & -1 & 34 & 31 & -1 & 14 & -1 & 4 & -1 & -1 & -1 & -1 & -1 & 22 & 24 \end{pmatrix} \tag{D.2}$$

Rate 3/4 LDPC code matrix

$$\begin{pmatrix} 35 & 19 & 41 & 22 & 40 & 41 & 39 & 6 & 28 & 18 & 17 & 3 & 28 & -1 & -1 & -1 \\ 29 & 30 & 0 & 8 & 33 & 22 & 17 & 4 & 27 & 28 & 20 & 27 & 24 & 23 & -1 & -1 \\ 37 & 31 & 18 & 23 & 11 & 21 & 6 & 20 & 32 & 9 & 12 & 29 & -1 & 0 & 13 & -1 \\ 25 & 22 & 4 & 34 & 31 & 3 & 14 & 15 & 4 & -1 & 14 & 18 & 13 & 13 & 22 & 24 \end{pmatrix} \tag{D.3}$$

Rate 13/16 LDPC code matrix

$$\begin{pmatrix} 29 & 30 & 0 & 8 & 33 & 22 & 17 & 4 & 27 & 28 & 20 & 27 & 24 & 23 & -1 & -1 \\ 37 & 31 & 18 & 23 & 11 & 21 & 6 & 20 & 32 & 9 & 12 & 29 & 10 & 0 & 13 & -1 \\ 25 & 22 & 4 & 34 & 31 & 3 & 14 & 15 & 4 & 2 & 14 & 18 & 13 & 13 & 22 & 24 \end{pmatrix} \tag{D.4}$$

## D.2 Reed Solomon (N,K)

Reed–Solomon codes are a group of error-correcting [6].It is able to detect and correct multiple symbol errors. By adding t check symbols to the data, a Reed–Solomon code can detect any combination of up to t erroneous symbols, or correct up to $\lfloor t/2 \rfloor$ symbols. As an erasure code, it can correct up to t known erasures, or it can detect and correct combinations of errors and erasures. Furthermore, Reed–Solomon codes are suitable as multiple-burst bit-error correcting codes, since a sequence of b + 1 consecutive bit errors can affect at most two symbols of size b. The choice of t is up to the designer of the code, and may be selected within wide limits.

The Reed–Solomon code is a linear block code of length n with dimension k and minimum Hamming distance n-k+1. The Reed–Solomon code is optimal in the sense that the minimum distance has the maximum value possible for a linear code of size (n, k). The error-correcting ability of a Reed–Solomon code is determined by its minimum distance, or equivalently, by n-k , the measure of redundancy in the block. It is able to correct errors which are known in advance by side information from the

demodulator.

Reed–Solomon codes, it is common to use a finite field with $2^m$ elements. In this case, each symbol can be represented as an 8-bit value to make the encoder byte-oriented computer systems.) The Reed–Solomon code properties discussed above make them especially well-suited to applications where errors occur in bursts. This is because it does not matter to the code how many bits in a symbol are in error — if multiple bits in a symbol are corrupted it only counts as a single error. Conversely, if a data stream is not characterized by error bursts or drop-outs but by random single bit errors, a Reed–Solomon code is usually a poor choice compared to a binary code.

### D.2.1 Encoding

The word is coded with the polynomial fixed by the standard which is shown:

$$g(x) = \prod_{k=1}^{16} = (x + \alpha^k) \tag{D.5}$$

where $\alpha$ = 0x02 is a root of the primitive polynomial p(x) = $1 + x^2 + x^3 + x^4 + x^8$.

The words are fragmented in groups of 8 bits (bytes) named as m vector in a GF($2^8$). The parity vector is calculated as:

$$r(x) = x^{16} m(x) mod g(x) \tag{D.6}$$

The codeword is formed appending the bits and the redundancy.

$$x = (m_{M-1}, m_{M-1}, ..., m_1, m_0, r_{n-k-1}, ..., r_0) \tag{D.7}$$

Where n is the size of the word and k the size of the codeword.

### D.2.2 Decoding

The transmitted code word is always divisible by the generator polynomial without remainder and that this property extends to the individual factors of the generator polynomial. Therefore the first step in the decoding process is to divide the received polynomial by each of the factors. Resulting in a reminder shown in the next formula:

$$\frac{R(x)}{x + \alpha^i} = Q_i(x) + \frac{S_i}{x + \alpha^i} \tag{D.8}$$

and the remainder (syndrome):

$$S_i = Q_i(x) \cdot (x + \alpha_i) + R(X) \tag{D.9}$$

substituting x = $\alpha^i$ in the received polynomial.

$$S_i = R_{n-1}(\alpha^i)^{n-1} + R_{n-2}(\alpha^i)^{n-2} + ... + R_1(\alpha^i) + R_0 \tag{D.10}$$

Once the syndromes are calculated, errors could be located in the terms whose coefficient is not null. It must be noticed that lack of error generates a zero polynomial syndrome. Calculating the inverse of the coefficients which are not null the error signal is reduces to zero.

## D.3 Block code (8,N)

Linear codes are traditionally partitioned into block codes [6]. Linear codes are used in forward error correction and are applied in methods for transmitting symbols on a communications channel so that, if errors occur in the communication, some errors can be corrected or detected by the recipient of a message block. The codewords in a linear block code are blocks of symbols that are encoded using more symbols than the original value to be sent.

The notation of this Block code is (N,X) where N is the size of the code and X the side of the codeword. The humming distance d = X-N, represent the number of errors which could be corrected $2^{r-2} - 1$.

### D.3.1 Encoding

The data stream is segmented in 8 bits block and multiplied by the generator matrix, appending the word with the redundancy.

$$c_{1xN} = b_{1x8} G_{8xN} \tag{D.11}$$

The generator matrices are the following ones:

$$G_{8X9} = \begin{pmatrix} 1 & 0 & 0 & 0 & 0 & 0 & 0 & 0 & 1 \\ 0 & 1 & 0 & 0 & 0 & 0 & 0 & 0 & 1 \\ 0 & 0 & 1 & 0 & 0 & 0 & 0 & 0 & 1 \\ 0 & 0 & 0 & 1 & 0 & 0 & 0 & 0 & 1 \\ 0 & 0 & 0 & 0 & 1 & 0 & 0 & 0 & 1 \\ 0 & 0 & 0 & 0 & 0 & 1 & 0 & 0 & 1 \\ 0 & 0 & 0 & 0 & 0 & 0 & 1 & 0 & 1 \\ 0 & 0 & 0 & 0 & 0 & 0 & 0 & 1 & 1 \end{pmatrix} \tag{D.12}$$

$$G_{8X12} = \begin{pmatrix} 1 & 0 & 0 & 0 & 0 & 0 & 0 & 0 & 1 & 1 & 0 & 0 \\ 0 & 1 & 0 & 0 & 0 & 0 & 0 & 0 & 1 & 0 & 1 & 0 \\ 0 & 0 & 1 & 0 & 0 & 0 & 0 & 0 & 0 & 1 & 0 & 1 \\ 0 & 0 & 0 & 1 & 0 & 0 & 0 & 0 & 0 & 0 & 1 & 1 \\ 0 & 0 & 0 & 0 & 1 & 0 & 0 & 0 & 1 & 0 & 1 & 1 \\ 0 & 0 & 0 & 0 & 0 & 1 & 0 & 0 & 1 & 1 & 0 & 1 \\ 0 & 0 & 0 & 0 & 0 & 0 & 1 & 0 & 1 & 1 & 1 & 0 \\ 0 & 0 & 0 & 0 & 0 & 0 & 0 & 1 & 0 & 1 & 1 & 1 \end{pmatrix} \tag{D.13}$$

$$G_{8X16} = \begin{pmatrix} 1 & 0 & 0 & 0 & 0 & 0 & 0 & 0 & 0 & 0 & 1 & 1 & 1 & 0 & 1 & 0 \\ 0 & 1 & 0 & 0 & 0 & 0 & 0 & 0 & 1 & 0 & 0 & 1 & 0 & 1 & 0 & 1 \\ 0 & 0 & 1 & 0 & 0 & 0 & 0 & 0 & 0 & 1 & 0 & 0 & 1 & 0 & 1 & 0 \\ 0 & 0 & 0 & 1 & 0 & 0 & 0 & 0 & 0 & 1 & 0 & 1 & 1 & 1 & 0 & 1 \\ 0 & 0 & 0 & 0 & 1 & 0 & 0 & 0 & 1 & 0 & 1 & 0 & 0 & 1 & 1 & 0 \\ 0 & 0 & 0 & 0 & 0 & 1 & 0 & 0 & 0 & 1 & 0 & 1 & 0 & 0 & 1 & 1 \\ 0 & 0 & 0 & 0 & 0 & 0 & 1 & 0 & 1 & 0 & 1 & 0 & 1 & 0 & 0 & 1 \\ 0 & 0 & 0 & 0 & 0 & 0 & 0 & 1 & 1 & 1 & 1 & 1 & 0 & 1 & 0 & 1 \end{pmatrix} \tag{D.14}$$

### D.3.2 Decoding

As it is presented in the Reed Solomon decoding section. A linear code can be decoding calculating the possible errors vector which could occur, the number of error vectors r syndromes depends on the size of the word and the codeword.

Depending on the size of the codewords the number of syndromes are calculated based on the inverse generation function calculated:

$$G = [P|I_k] \tag{D.15}$$

$$H = [I_{n-k}| - P^T] \tag{D.16}$$

After generating the syndromes the error must be detected. The input codewords are multiplied by the inverse generation function. As a result, if the vector obtained is null the input codewords belongs to the space of codewords or the error cannot be detected, but if it is not null an error is detected and it is compared with the syndromes generated.

The comparison with the syndromes must result in a coincidence, then the error pattern is know and the codeword can be corrected adding the error vector in module 2 correcting the codeword. The first 8 bits of each codeword are the data decoded.

# Appendix E

# Transmission procedures

## E.1 Spectrum Matching

The frequency operation band for this project is 60 GHz, it is not a regulated band. However, it is required to fulfill a mask in order to operate it. The former requirements are accomplished differently in each physical layer, in OFDM a windowing process is done and in the other physical layer root cosine filter is used.

### E.1.1 OFDM

The windowing function is used to smooth the transition between adjacent fields in the packet where OFDM modulation is employed. The windowing function is different from being equivalent to "1" only in the transition region. The transition region creates an overlap (with length TR) between adjacent fields. The field wave form is extended cyclically to fill the part of the transition region in which it is undefined. If the transition region vanishes, the windowing function degenerates to a rectangular window. The choice of windowing function is implementation dependent, as long as transmit EVM and transmit mask requirements are met.

### E.1.2 CL, SC, and LPSC

To the rest of the physical layers a root-raised cosine filter with roll-off of 0.25 is used to fulfill the mask and EVM requirements.

## E.2 Quantization and Packets Generation

8 bits quantization procedure is required in order to operate with the signal generator. This procedure introduces quantization error reducing accuracy due to the change to double resolution to 8 bits resolution.

In the transmitter, signal maximum value is used to normalize the signal and then is scaled in a range between -127 to 127. Afterwards, the signal is converted to 8 bit resolution values.

In the receiver, signal maximum value is obtained and used to denormalize the signal. Real and imaginary values of the signal are stored separately in order to keep the phase information.

The normalize signal is divided in real and imaginary values, the imaginary and real streams of data are stored in different 8 bits files.

## E.3 Resampling

Sampling procedure lets quantize continues domain signals [10]. The mathematical representation is:

$$x[n] = x_c(nT) \tag{E.1}$$

Signal generator sample rate may be different of the sample frequency standardized for the signal. Therefore, a change in the sample frequency rate is required to obtain a new discrete-time representation of the underlying continuous time signal of the form:

$$x^{`}[n] = x_c(nT^{`}) \tag{E.2}$$

However, there are involved other procedures such as D/A conversion, A/D conversion, consequently, it is not desired considered discrete-time operations exclusively. The conversion factor which is going to be considered is an integer factor. It may be considered a reduction case or down sampling procedure and expansion or up sampling procedure.

Down sampling (Decimation): Reduction of the sampling rate the expression for the discrete sequence is:

$$x_d[n] = x[nM] = x_c(nMT) \tag{E.3}$$

$X_d[n]$ is a replica of $x_c(t)$ if Nyquist requirements are accomplished. $\frac{\pi}{T'} = \frac{\pi}{MT}$ > Fmax. It can be inferred that the sample frequency must be at least M times the original sample frequency.

Up sampling (Interpolation): A reduction of the sampling rate is equivalent to sampling a continuous signal. However, increasing the sampling rate is related with the interpolation which is accomplished in a D/C conversion. Considering the expression of the continues signal sampled and the single obtained after increasing the sample rate the equations obtained are shown in the Figure E.1.

$$x_d[n] = x[\frac{n}{L}] = x_c(n\frac{T}{L}) \tag{E.4}$$

In order to accomplished the bandwidth required and the Nyquist conditions the following filtering system is used.

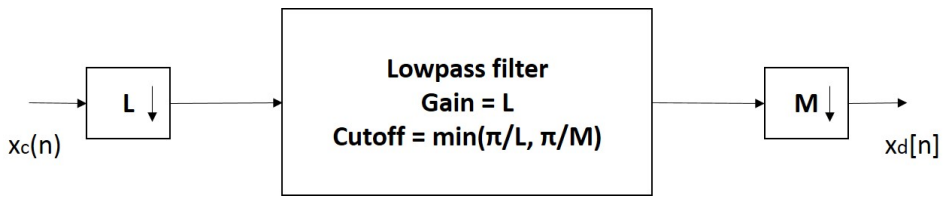


FIGURE E.1: Resampling scheme.

# Appendix F

# Modulations

This appendix is intended to shown the constellations of the different constellations and the amplitude level of each symbol.

The DBPSK constellation is shown in Figure F.1.

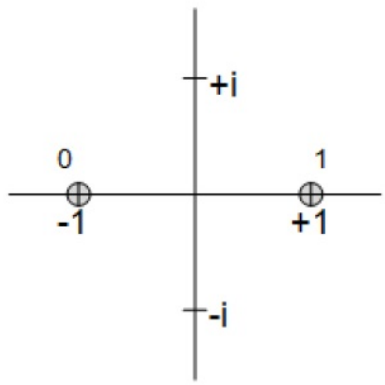


FIGURE F.1: DBPSK constellation.

The $\frac{\pi}{2}$ - BPSK constellation is equal to the DBPSK constellation, but the symbols are rotated -$\frac{\pi}{2}$. Therefore, the symbol 1 has an amplitude of -j and the symbol 0 an amplitude of j.

The $\frac{\pi}{2}$ - QPSK constellation is shown in Figure F.2.

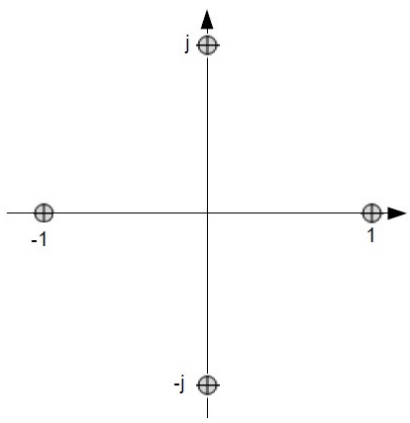


FIGURE F.2: $\frac{\pi}{2}$ - QPSK constellation.

The $\frac{\pi}{2}$ - 16-QAM constellation is shown in Figure F.3.

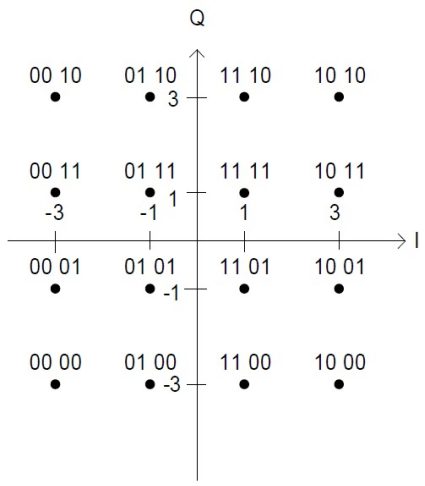


FIGURE F.3: $\frac{\pi}{2}$ - 16-QAM constellation.

The $\frac{\pi}{2}$ - 64-QAM constellation is shown in Figure F.4.

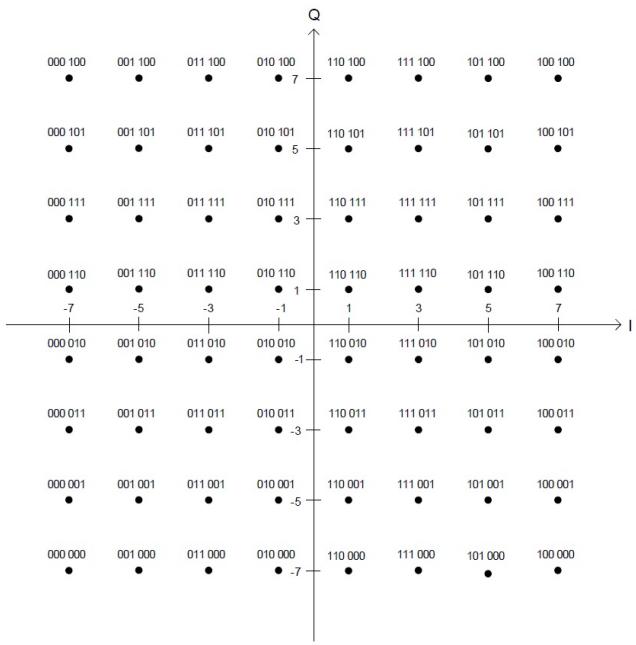


FIGURE F.4: 64-QAM constellation.